UNIVERSIDAD DE BARCELONA

FACULTAD DE FARMACIA

**DEPARTAMENTO
BIOQUIMICA Y BIOLOGIA MOLECULAR**

PREDICCIÓN DE RESPUESTA AL TRATAMIENTO EN PACIENTES CON CARCINOMA ESCAMOSO DE CABEZA Y CUELLO

**MIGUEL ANGEL PAVÓN RIBAS
2009**

IX. ANEXOS

IX ANEXOS

ANEXO 1. Genes expresados diferencialmente al comparar los tumores del cluster 1 con los tumores del cluster 2 y 3

ANEXO 2. Genes expresados diferencialmente al comparar los tumores del cluster 3 con los tumores del cluster 1 y 2

ANEXO 3. Genes expresados diferencialmente al comparar los tumores del cluster 2 con los tumores del cluster 1 y 3

ANEXO 4. Genes expresados diferencialmente en función de la rediviva local a los 2 años

ANEXO 5. Genes expresados diferencialmente en función de la supervivencia a 3 años

ANEXO 6. Genes expresados diferencialmente en función de la respuesta a la quimioterapia de inducción

ANEXO 7. Genes expresados diferencialmente tras comparar los niveles de expresión de los tumores respecto a las mucosas normales

ANEXO 8. Publicación de los resultados obtenidos en el estudio de los niveles de expresión de los genes del sistema NHEJ en biopsias pre-tratamiento de pacientes con carcinoma escamosos de cabeza y cuello localmente avanzado tratados con quimioterapia de inducción (Int J Cancer. 2008 Sep 1;123(5):1068-79)

ANEXO 1: Genes expresados diferencialmente al comparar los tumores del cluster 1 con los tumores del cluster 2 y 3 (p ajustada<0,05)

Probe	Symbol	Description	Cytoband	t-statistic	p-value	adjp
202627_s_at	SERPINE1	serpin peptidase inhibitor, clade E (nexin, plasminogen activator inhibitor type 1), member 1	7q21.3-q22	6.84534	1e-04	9e-04
201109_s_at	THBS1	thrombospondin 1	15q15	6.77397	1e-04	9e-04
210511_s_at	INHBA	inhibin, beta A	7p15-p13	6.76322	1e-04	9e-04
212473_s_at	MICAL2	microtubule associated monoxygenase, calponin and LIM domain containing 2	11p15.3	6.53966	1e-04	0.0017
221471_at	SERINC3	serine incorporator 3	20q13.1-q13.3	6.48186	1e-04	0.0023
202620_s_at	PLOD2	procollagen-lysine, 2-oxoglutarate 5-dioxygenase 2	3q23-q24	6.43661	1e-04	0.0026
201105_at	LGALS1	lectin, galactoside-binding, soluble, 1 (galectin 1)	22q13.1	6.35539	1e-04	0.0035
202949_s_at	FHL2	four and a half LIM domains 2	2q12-q14	6.20728	1e-04	0.0061
211945_s_at	ITGB1	integrin, beta 1 (fibronectin receptor, beta polypeptide, antigen CD29 includes MDF2, MSK12)	10p11.2	6.16237	1e-04	0.0074
201108_s_at	THBS1	thrombospondin 1	15q15	6.10825	1e-04	0.0087
203889_at	SCG5	secretogranin V (7B2 protein)	15q13-q14	6.09843	1e-04	0.0089
202619_s_at	PLOD2	procollagen-lysine, 2-oxoglutarate 5-dioxygenase 2	3q23-q24	6.03842	1e-04	0.0102
207543_s_at	P4HA1	procollagen-proline, 2-oxoglutarate 4-dioxygenase (proline 4-hydroxylase), alpha polypeptide I	10q21.3-q23.1	5.99899	2e-04	0.0114
219655_at	C7orf10	chromosome 7 open reading frame 10	7p14.1	5.99055	1e-04	0.0117
203735_x_at	PPFIBP1	PTPRF interacting protein, binding protein 1 (liprin beta 1)	12p11.23-p11.22	5.87329	1e-04	0.0175
222235_s_at	GALNACT-2	chondroitin sulfate GalNAcT-2	10q11.21	5.85546	1e-04	0.0182
204140_at	TPST1	tyrosylprotein sulfotransferase 1	7q11.21	5.82066	1e-04	0.0197
218368_s_at	TNFRSF12A	tumor necrosis factor receptor superfamily, member 12A	16p13.3	5.79667	1e-04	0.0212
200755_s_at	CALU	calumenin	7q32	5.79539	1e-04	0.0212
212472_at	MICAL2	microtubule associated monoxygenase, calponin and LIM domain containing 2	11p15.3	5.72337	1e-04	0.0253
206026_s_at	TNFAIP6	tumor necrosis factor, alpha-induced protein 6	2q23.3	5.72057	1e-04	0.0256
203736_s_at	PPFIBP1	PTPRF interacting protein, binding protein 1 (liprin beta 1)	12p11.23-p11.22	5.64557	1e-04	0.0335
212097_at	CAV1	caveolin 1, caveolae protein, 22kDa	7q31.1	5.62559	1e-04	0.036
218618_s_at	FNDC3B	fibronectin type III domain containing 3B	3q26.31	5.62314	1e-04	0.0361

Probe ID	Symbol	Gene name	Location	Value		p-value
203065_s_at	CAV1	caveolin 1, caveolae protein, 22kDa	7q31.1	5.60839	1e-04	0.0375
201110_s_at	THBS1	thrombospondin 1	15q15	5.60554	1e-04	0.0377
214845_s_at	CALU	calumenin	7q32	5.56538	1e-04	0.0425
209935_at	ATP2C1	ATPase, Ca++ transporting, type 2C, member 1	3q22.1	5.53188	1e-04	0.0469
202395_at	NSF	N-ethylmaleimide-sensitive factor	17q21	-5.52875	1e-04	0.047
203914_x_at	HPGD	hydroxyprostaglandin dehydrogenase 15-(NAD)	4q34-q35	-5.58465	1e-04	0.0405
213236_at	SASH1	SAM and SH3 domain containing 1	6q24.3	-5.5882	1e-04	0.0398
37201_at	ITIH4	inter-alpha (globulin) inhibitor H4 (plasma Kallikrein-sensitive glycoprotein)	3p21-p14	-5.61257	1e-04	0.037
219727_at	DUOX2	dual oxidase 2	15q15.3	-5.79467	1e-04	0.0212
209389_x_at	DBI	diazepam binding inhibitor (GABA receptor modulator, acyl-Coenzyme A binding protein)	2q12-q21	-5.82948	1e-04	0.0191
218186_at	RAB25	RAB25, member RAS oncogene family	1q22	-5.84865	1e-04	0.0183
220017_x_at	CYP2C9	cytochrome P450, family 2, subfamily C, polypeptide 9	10q24	-5.89195	1e-04	0.0166
206004_at	TGM3	transglutaminase 3 (E polypeptide, protein-glutamine-gamma-glutamyltransferase)	20q11.2	-5.92236	1e-04	0.0154
41644_at	SASH1	SAM and SH3 domain containing 1	6q24.3	-5.93358	1e-04	0.0143
207935_s_at	KRT13	keratin 13	17q12-q21.2	-6.02933	1e-04	0.0107
213929_at				-6.12136	1e-04	0.0083
211070_x_at	DBI	diazepam binding inhibitor (GABA receptor modulator, acyl-Coenzyme A binding protein)	2q12-q21	-6.46266	1e-04	0.0025
202428_x_at	DBI	diazepam binding inhibitor (GABA receptor modulator, acyl-Coenzyme A binding protein)	2q12-q21	-6.50324	1e-04	0.002
205379_at	CBR3	carbonyl reductase 3	21q22.2	-6.54964	1e-04	0.0017
208126_s_at	CYP2C18	cytochrome P450, family 2, subfamily C, polypeptide 18	10q24	-6.73238	1e-04	0.0011
212841_s_at	PPFIBP2	PTPRF interacting protein, binding protein 2 (liprin beta 2)	11p15.4	-6.80413	1e-04	9e-04
215103_at	CYP2C18	cytochrome P450, family 2, subfamily C, polypeptide 18	10q24	-7.60674	1e-04	1e-04
214070_s_at	ATP10B	ATPase, Class V, type 10B	5q34	-7.63	1e-04	1e-04

ANEXO 2: Genes expresados diferencialmente al comparar los tumores del cluster 3 con los tumores del cluster 1 y 2 (p ajustada<0,05)

Probe	Symbol	Description	Cytoband	t-statistic	p-value	adjp
211597_s_at	HOP	homeodomain-only protein	4q11-q12	8.57654	1e-04	1e-04
204952_at	LYPD3	LY6/PLAUR domain containing 3	19q13.31	8.44235	1e-04	1e-04
214536_at	SLURP1	secreted LY6/PLAUR domain containing 1	8q24.3	8.34153	1e-04	1e-04
205185_at	SPINK5	serine peptidase inhibitor, Kazal type 5	5q32	7.81475	1e-04	1e-04
220620_at	CRCT1	cysteine-rich C-terminal 1	1q21	7.69724	1e-04	1e-04
206125_s_at	KLK8	kallikrein-related peptidase 8	19q13.3-q13.4	7.41616	1e-04	1e-04
219529_at	CLIC3	chloride intracellular channel 3	9q34.3	7.32736	1e-04	1e-04
220413_at	SLC39A2	solute carrier family 39 (zinc transporter), member 2	14q11.2	7.02418	1e-04	2e-04
203747_at	AQP3	aquaporin 3 (Gill blood group)	9p13	6.49846	1e-04	6e-04
204971_at	CSTA	cystatin A (stefin A)	3q21	6.42767	1e-04	0.001
219554_at	RHCG	Rh family, C glycoprotein	15q25	6.42418	1e-04	0.0011
39248_at	AQP3	aquaporin 3 (Gill blood group)	9p13	6.2454	1e-04	0.0023
219722_s_at	GDPD3	glycerophosphodiester phosphodiesterase domain containing 3	16p11.2	6.20168	1e-04	0.0029
212657_s_at	IL1RN	interleukin 1 receptor antagonist	2q14.2	6.19893	1e-04	0.0029
205778_at	KLK7	kallikrein-related peptidase 7	19q13.33	6.17859	1e-04	0.0031
39249_at	AQP3	aquaporin 3 (Gill blood group)	9p13	6.12927	1e-04	0.004
205759_s_at	SULT2B1	sulfotransferase family, cytosolic, 2B, member 1	19q13.3	6.07189	1e-04	0.0048
219597_s_at	DUOX1	dual oxidase 1	15q15.3	6.04634	1e-04	0.0051
206884_s_at	SCEL	sciellin	13q22	5.94222	1e-04	0.0082
207602_at	TMPRSS11D	transmembrane protease, serine 11D	4q13.2	5.925	1e-04	0.0087
222223_s_at	IL1F5	interleukin 1 family, member 5 (delta)	2q14	5.8776	1e-04	0.01
203021_at	SLPI	secretory leukocyte peptidase inhibitor	20q12	5.85279	1e-04	0.0112
203407_at	PPL	periplakin	16p13.3	5.85159	1e-04	0.0112
214599_at	IVL	involucrin	1q21	5.84761	1e-04	0.0112
206008_at	TGM1	transglutaminase 1 (K polypeptide epidermal type I, protein-glutamine-gamma-glutamyltransferase)	14q11.2	5.81622	1e-04	0.0122
201201_at	CSTB	cystatin B (stefin B)	21q22.3	5.77212	1e-04	0.0132
214838_at	SFT2D2	SFT2 domain containing 2	1q24.2	5.74449	1e-04	0.0148

Probe ID	Gene Symbol	Gene Name	Location	Score	p-value	q-value
221665_s_at	EPS8L1	EPS8-like 1	19q13.42	5.72572	1e-04	0.0157
210397_at	DEFB1	defensin, beta 1	8p23.2-p23.1	5.71318	1e-04	0.0162
205470_s_at	KLK11	kallikrein-related peptidase 11	19q13.3-q13.4	5.70406	1e-04	0.017
266_s_at	CD24	CD24 molecule	6q21	5.69613	1e-04	0.0174
221667_s_at	HSPB8	heat shock 22kDa protein 8	12q24.23	5.64864	1e-04	0.0214
208650_s_at	CD24	CD24 molecule	6q21	5.63916	1e-04	0.0222
206400_at	LGALS7	lectin, galactoside-binding, soluble, 7 (galectin 7)	19q13.2	5.6206	1e-04	0.0234
201939_at	PLK2	polo-like kinase 2 (Drosophila)	5q12.1-q13.2	5.61335	1e-04	0.0243
218853_s_at	MOSPD1	motile sperm domain containing 1	Xq26.3	5.59377	1e-04	0.0255
205627_at	CDA	cytidine deaminase	1p36.2-p35	5.54196	1e-04	0.0301
209792_s_at	KLK10	kallikrein-related peptidase 10	19q13.3-q13.4	5.51862	1e-04	0.0323
210128_s_at	LTB4R	leukotriene B4 receptor	14q11.2-q12	5.51518	1e-04	0.0326
204733_at	KLK6	kallikrein-related peptidase 6	19q13.3	5.5139	1e-04	0.0327
220782_x_at	KLK12	kallikrein-related peptidase 12	19q13.3-q13.4	5.51209	1e-04	0.0329
205863_at	S100A12	S100 calcium binding protein A12	1q21	5.51139	1e-04	0.0329
214549_x_at	SPRR1A	small proline-rich protein 1A	1q21-q22	5.51016	1e-04	0.0329
222242_s_at	KLK5	kallikrein-related peptidase 5	19q13.3-q13.4	5.5089	1e-04	0.0331
209800_at	KRT16	keratin 16 (focal non-epidermolytic palmoplantar keratoderma)	17q12-q21	5.50785	1e-04	0.0332
220412_x_at	KCNK7	potassium channel, subfamily K, member 7	11q13	5.46109	1e-04	0.0372
201454_s_at	NPEPPS	aminopeptidase puromycin sensitive	17q21	5.45814	1e-04	0.0373
205363_at	BBOX1	butyrobetaine (gamma), 2-oxoglutarate dioxygenase (gamma-butyrobetaine hydroxylase) 1	11p14.2	5.45565	1e-04	0.0373
206605_at	P11	26 serine protease	12q13.1	5.43246	1e-04	0.0406
218779_x_at	EPS8L1	EPS8-like 1	19q13.42	5.42746	1e-04	0.0414
205783_at	KLK13	kallikrein-related peptidase 13	19q13.3-q13.4	5.41887	1e-04	0.0429
203535_at	S100A9	S100 calcium binding protein A9	1q21	5.39759	1e-04	0.0455
206199_at	CEACAM7	carcinoembryonic antigen-related cell adhesion molecule 7	19q13.2	5.38961	1e-04	0.0464
213680_at	KRT6C	keratin 6C	12q13.13	5.38696	1e-04	0.0465
218186_at	RAB25	RAB25, member RAS oncogene family	1q22	5.37569	1e-04	0.0485
91826_at	EPS8L1	EPS8-like 1	19q13.42	5.3675	1e-04	0.049

ANEXO 3: Genes expresados diferencialmente al comparar los tumores del cluster 2 con los tumores del cluster 1 y 3 (p ajustada<0,05)

Probe	Symbol	Description	Cytoband	t-statistic	p-value	adjp
201650_at	KRT19	keratin 19	17q21.2	6.65757	1e-04	2e-04
218440_at	MCCC1	methylcrotonoyl-Coenzyme A carboxylase 1 (alpha)	3q27	6.08479	1e-04	0.0015
209205_s_at	LMO4	LIM domain only 4	1p22.3	6.03463	1e-04	0.002
218546_at	C1orf115	chromosome 1 open reading frame 115	1q41	5.78374	1e-04	0.0062
201908_at	DVL3	dishevelled, dsh homolog 3 (Drosophila)	3q27	5.39203	1e-04	0.026
204734_at	KRT15	keratin 15	17q21.2	5.19762	1e-04	0.0499
208636_at	ACTN1	actinin, alpha 1	14q24.1-q24.2 14q24 14q22-q24	-5.24627	1e-04	0.043
208898_at	ATP6V1D	ATPase, H+ transporting, lysosomal 34kDa, V1 subunit D	14q23-q24.2	-5.25764	1e-04	0.041
202693_s_at	STK17A	serine/threonine kinase 17a	7p12-p14	-5.40438	1e-04	0.0251
203234_at	UPP1	uridine phosphorylase 1	7p12.3	-5.43455	1e-04	0.0233
200985_s_at	CD59	CD59 molecule, complement regulatory protein	11p13	-5.51034	1e-04	0.0186
208899_x_at	ATP6V1D	ATPase, H+ transporting, lysosomal 34kDa, V1 subunit D	14q23-q24.2	-5.54391	1e-04	0.0163
205627_at	CDA	cytidine deaminase	1p36.2-p35	-5.56329	1e-04	0.0151
219165_at	PDLIM2	PDZ and LIM domain 2 (mystique)	8p21.2	-5.5657	1e-04	0.015
215813_s_at	PTGS1	prostaglandin-endoperoxide synthase 1 (prostaglandin G/H synthase and cyclooxygenase)	9q32-q33.3	-5.65713	1e-04	0.0104
217873_at	CAB39	calcium binding protein 39	2q37.1	-5.66127	1e-04	0.0103
205767_at	EREG	epiregulin	4q13.3	-5.68622	1e-04	0.0091
209946_at	VEGFC	vascular endothelial growth factor C	4q34.1-q34.3	-5.76699	1e-04	0.007
218644_at	PLEK2	pleckstrin 2	14q23.3	-5.8055	1e-04	0.0055
202949_s_at	FHL2	four and a half LIM domains 2	2q12-q14	-6.02845	1e-04	0.0021
210138_at	RGS20	regulator of G-protein signaling 20	8q12.1	-6.37452	1e-04	4e-04
201939_at	PLK2	polo-like kinase 2 (Drosophila)	5q12.1-q13.2	-6.49047	1e-04	4e-04

ANEXO 4: Genes expresados diferencialmente en función de la recidiva local a los 2 años (p<0,001)

Probe	Symbol	Description	Cytoband	t-statistic	p-value	adjp
217993_s_at	MAT2B	methionine adenosyltransferase II, beta	5q34-q35.1	4.57716	2e-04	0.4089
200748_s_at	FTH1	ferritin, heavy polypeptide 1	11q13	4.36626	3e-04	0.5913
217865_at	RNF130	ring finger protein 130	5q35.3	4.24456	3e-04	0.7005
207277_at	CD209	CD209 molecule	19p13	4.2225	5e-04	0.7176
219318_x_at	MED31	mediator complex subunit 31	17p13.2	4.13949	2e-04	0.7866
206129_s_at	ARSB	arylsulfatase B	5q11-q13	4.13633	7e-04	0.7885
209287_s_at	CDC42EP3	CDC42 effector protein (Rho GTPase binding) 3	2p21	4.06079	4e-04	0.8417
37986_at	EPOR	erythropoietin receptor	19p13.3-p13.2	4.04038	4e-04	0.8536
208964_s_at	FADS1	fatty acid desaturase 1	11q12.2-q13.1	3.93975	1e-04	0.9101
209288_s_at	CDC42EP3	CDC42 effector protein (Rho GTPase binding) 3	2p21	3.9137	9e-04	0.9242
214211_at	FTH1	ferritin, heavy polypeptide 1	11q13	3.91065	3e-04	0.9249
208354_s_at	SLC12A3	solute carrier family 12 (sodium/chloride transporters), member 3	16q13	3.90894	3e-04	0.9256
218852_at	PPP2R3C	protein phosphatase 2 (formerly 2A), regulatory subunit B'', gamma	14q13.2	3.89281	4e-04	0.9308
202623_at	EAPP	E2F-associated phosphoprotein	14q13.1	3.89032	6e-04	0.9313
204185_x_at	PPID	peptidylprolyl isomerase D (cyclophilin D)	4q31.3	3.88913	4e-04	0.9318
202892_at	CDC23	cell division cycle 23 homolog (S. cerevisiae)	5q31	3.86145	4e-04	0.9418
204140_at	TPST1	tyrosylprotein sulfotransferase 1	7q11.21	3.84704	3e-04	0.9457
200013_at	RPL24	ribosomal protein L24	3q12	3.83201	9e-04	0.9511
201330_at	RARS	arginyl-tRNA synthetase	5q35.1	3.81124	3e-04	0.9584
204349_at	MED7	mediator complex subunit 7	5q33.3	3.8074	7e-04	0.9592
208198_x_at	KIR2DS1	killer cell immunoglobulin-like receptor, two domains, short cytoplasmic tail, 1	19q13.4	3.79564	8e-04	0.9624
209046_s_at	GABARAPL2	GABA(A) receptor-associated protein-like 2	16q22.3-q24.1	3.79255	5e-04	0.9629
200730_s_at	PTP4A1	protein tyrosine phosphatase type IVA, member 1	6q12	3.77523	8e-04	0.9669
201503_at	G3BP1	GTPase activating protein (SH3 domain) binding protein 1	5q33.1	3.72947	9e-04	0.9783
206307_s_at	FOXD1	forkhead box D1	5q12-q13	3.70576	6e-04	0.9814
221597_s_at	HSPC171	HSPC171 protein	16q22.1	3.7056	7e-04	0.9814
218339_at	MRPL22	mitochondrial ribosomal protein L22	5q33.1-q33.3	3.68198	8e-04	0.9848

Probe ID	Gene Symbol	Gene Name	Cytoband	Value	p-value	Score
220416_at	ATP8B4	ATPase, Class I, type 8B, member 4	15q21.2	3.67825	4e-04	0.985
201272_at	AKR1B1	aldo-keto reductase family 1, member B1 (aldose reductase)	7q35	3.65533	7e-04	0.9874
209181_s_at	RABGGTB	Rab geranylgeranyltransferase, beta subunit	1p31	3.64813	4e-04	0.9883
210278_s_at	AP4S1	adaptor-related protein complex 4, sigma 1 subunit	14q12	3.60072	9e-04	0.993
221423_s_at	YIPF5	Yip1 domain family, member 5	5q32	3.58151	9e-04	0.9946
211671_s_at	NR3C1	nuclear receptor subfamily 3, group C, member 1 (glucocorticoid receptor)	5q31.3	3.55595	8e-04	0.996
220332_at	CLDN16	claudin 16	3q28	3.55025	8e-04	0.9965
204191_at	IFNAR1	interferon (alpha, beta and omega) receptor 1	21q22.1 21q22.11	3.51619	5e-04	0.9976
217585_at	NEBL	nebulette	10p12	-3.08968	9e-04	1
221507_at	TNPO2	transportin 2 (importin 3, karyopherin beta 2b)	19p13.13	-3.25633	8e-04	0.9999
215063_x_at	LRRC40	leucine rich repeat containing 40	1p31.1	-3.48182	9e-04	0.9982
215404_x_at	FGFR1	fibroblast growth factor receptor 1 (fms-related tyrosine kinase 2, Pfeiffer syndrome)	8p11.2-p11.1	-3.53747	7e-04	0.9969
208965_s_at	PYHIN1	pyrin and HIN domain family, member 1	1q23.1	-3.6141	3e-04	0.9922
202725_at	POLR2A	polymerase (RNA) II (DNA directed) polypeptide A, 220kDa	17p13.1	-3.6203	8e-04	0.9912
214594_x_at	ATP8B1	ATPase, Class I, type 8B, member 1	18q21-q22 18q21.31	-3.63359	9e-04	0.9898
203546_at	IPO13	importin 13	1p34.1	-3.64354	7e-04	0.9886
210421_s_at	SLC24A1	solute carrier family 24 (sodium/potassium/calcium exchanger), member 1	15q22	-3.6651	3e-04	0.9862
220720_x_at	FAM128B	family with sequence similarity 128, member B	2q21.1	-3.68598	9e-04	0.9841
221506_s_at	TNPO2	transportin 2 (importin 3, karyopherin beta 2b)	19p13.13	-3.70103	4e-04	0.9818
212280_x_at	ATG4B	ATG4 autophagy related 4 homolog B (S. cerevisiae)	2q37.3	-3.70414	9e-04	0.9814
220659_s_at	C7orf43	chromosome 7 open reading frame 43	7q22.1	-3.72321	9e-04	0.9796
221071_at				-3.75331	3e-04	0.9719
215455_at	TIMELESS	timeless homolog (Drosophila)	12q12-q13	-3.92562	3e-04	0.9181
212051_at	WIPF2	WAS/WASL interacting protein family, member 2	17q21.2	-3.94179	3e-04	0.9092
200098_s_at	ANAPC5	anaphase promoting complex subunit 5	12q24.31	-3.94641	3e-04	0.9078
222159_at	PLXNA2	plexin A2	1q32.2	-4.0328	5e-04	0.8582
211950_at	UBR4	ubiquitin protein ligase E3 component n-recognin 4	1p36.13	-4.04228	3e-04	0.8521

Probe	Gene	Description	Cytoband			
202424_at	MAP2K2	mitogen-activated protein kinase kinase 2	19p13.3	-4.08718	4e-04	0.825
204292_x_at	STK11	serine/threonine kinase 11	19p13.3	-4.14233	4e-04	0.7846
218819_at	INTS6	integrator complex subunit 6	13q14.12-q14.2	-4.29471	3e-04	0.6553
220113_x_at	POLR1B	polymerase (RNA) I polypeptide B, 128kDa	2q13	-4.47848	2e-04	0.4907
221610_s_at	STAP2	signal transducing adaptor family member 2	19p13.3	-4.68134	1e-04	0.3335
218758_s_at	RRP1	ribosomal RNA processing 1 homolog (S. cerevisiae)	21q22.3	-4.8182	2e-04	0.2496

ANEXO 5. Genes expresados diferencialmente en función de la supervivencia a 3 años (p<0,001)

Probe	Symbol	Description	Cytoband	t-statistic	p-value	adjp
211828_s_at	TNIK	TRAF2 and NCK interacting kinase	3q26.2-q26.31	4.42673	1e-04	0.759
217993_s_at	MAT2B	methionine adenosyltransferase II, beta	5q34-q35.1	4.41078	3e-04	0.7694
207329_at	MMP8	matrix metallopeptidase 8 (neutrophil collagenase)	11q22.3	4.38759	3e-04	0.7852
204160_s_at	ENPP4	ectonucleotide pyrophosphatase/phosphodiesterase 4 (putative function)	6p12.3	4.35355	4e-04	0.806
204081_at	NRGN	neurogranin (protein kinase C substrate, RC3)	11q24	4.264	6e-04	0.8608
201272_at	AKR1B1	aldo-keto reductase family 1, member B1 (aldose reductase)	7q35	4.25977	2e-04	0.8628
209735_at	ABCG2	ATP-binding cassette, sub-family G (WHITE), member 2	4q22	4.23155	1e-04	0.8778
209683_at	FAM49A	family with sequence similarity 49, member A	2p24.3	4.18493	3e-04	0.9011
208092_s_at	FAM49A	family with sequence similarity 49, member A	2p24.3	4.09605	5e-04	0.937
203988_s_at	FUT8	fucosyltransferase 8 (alpha (1,6) fucosyltransferase)	14q24.3	4.08292	4e-04	0.9408
209122_at	ADFP	adipose differentiation-related protein	9p22.1	4.08128	3e-04	0.9415
222157_s_at	WDR48	WD repeat domain 48	3p21.33	4.07736	5e-04	0.9432
213712_at	ELOVL2	elongation of very long chain fatty acids (FEN1/Elo2, SUR4/Elo3, yeast)-like 2	6p24.2	4.01631	3e-04	0.9608
210004_at	OLR1	oxidized low density lipoprotein (lectin-like) receptor 1	12p13.2-p12.3	3.8986	5e-04	0.9839
204161_s_at	ENPP4	ectonucleotide pyrophosphatase/phosphodiesterase 4 (putative function)	6p12.3	3.89224	9e-04	0.9846
207794_at	CCR2	chemokine (C-C motif) receptor 2	3p21.31	3.88967	3e-04	0.9849
205404_at	HSD11B1	hydroxysteroid (11-beta) dehydrogenase 1	1q32-q41	3.88643	3e-04	0.9855
213515_x_at	HBG2	hemoglobin, gamma G	11p15.5	3.83116	8e-04	0.9909
210650_s_at	PCLO	piccolo (presynaptic cytomatrix protein)	7q11.23-q21.3	3.80343	9e-04	0.9935
216014_s_at	ZXDB	zinc finger, X-linked, duplicated B	Xp11.21	3.79658	6e-04	0.9937
213484_at				3.75909	4e-04	0.9952
204848_x_at	HBG1	hemoglobin, gamma A	11p15.5	3.71573	1e-04	0.9967
210288_at	KLRG1	killer cell lectin-like receptor subfamily G, member 1	12p12-p13	3.71153	2e-04	0.9971
213109_at	TNIK	TRAF2 and NCK interacting kinase	3q26.2-q26.31	3.66712	6e-04	0.9984

Probe ID	Gene	Description	Cytoband			
219924_s_at	ZMYM6	zinc finger, MYM-type 6	1p34.2	3.63951	7e-04	0.9988
206834_at	HBD	hemoglobin, delta	11p15.5	3.4221	5e-04	1
220807_at	HBQ1	hemoglobin, theta 1	16p13.3	3.35742	5e-04	1
213245_at	ADCY1	adenylate cyclase 1 (brain)	7p13-p12	3.26561	9e-04	1
210127_at	RAB6B	RAB6B, member RAS oncogene family	3q22.1	3.24361	2e-04	1
221427_s_at	CCNL2	cyclin L2	1p36.33	-3.38126	9e-04	1
200621_at	CSRP1	cysteine and glycine-rich protein 1	1q32	-3.48745	8e-04	0.9999
204251_s_at	CEP164	centrosomal protein 164kDa	11q23.3	-3.5084	6e-04	0.9999
202115_s_at	NOC2L	nucleolar complex associated 2 homolog (S. cerevisiae)	1p36.33	-3.51549	9e-04	0.9998
202774_s_at	SFRS8	splicing factor, arginine/serine-rich 8 (suppressor-of-white-apricot homolog, Drosophila)	12q24.33	-3.52184	9e-04	0.9998
202039_at	TIAF1	TGFB1-induced anti-apoptotic factor 1	17q11.2	-3.54987	9e-04	0.9997
221794_at	DOCK6	dedicator of cytokinesis 6	19p13.2	-3.57295	9e-04	0.9996
220402_at	P53AIP1	p53-regulated apoptosis-inducing protein 1	11q24	-3.58154	4e-04	0.9996
217950_at	NOSIP	nitric oxide synthase interacting protein	19q13.33	-3.58331	9e-04	0.9995
214695_at	UBAP2L	ubiquitin associated protein 2-like	1q21.3	-3.59096	5e-04	0.9994
215909_x_at	MINK1	misshapen-like kinase 1 (zebrafish)	17p13.2	-3.63189	4e-04	0.999
208874_x_at	PPP2R4	protein phosphatase 2A activator, regulatory subunit 4	9q34	-3.7016	9e-04	0.9975
211282_x_at	TNFRSF25	tumor necrosis factor receptor superfamily, member 25	1p36.2	-3.74146	9e-04	0.9961
38269_at	PRKD2	protein kinase D2	19q13.3	-3.77634	9e-04	0.9949
213812_s_at	CAMKK2	calcium/calmodulin-dependent protein kinase kinase 2, beta	12q24.2	-3.78385	9e-04	0.9944
201979_s_at	PPP5C	protein phosphatase 5, catalytic subunit	19q13.3	-3.78944	6e-04	0.9939
200695_at	PPP2R1A	protein phosphatase 2 (formerly 2A), regulatory subunit A, alpha isoform	19q13.33	-3.81826	5e-04	0.9921
204141_at	TUBB2A	tubulin, beta 2A	6p25	-3.81892	7e-04	0.992
211002_s_at	TRIM29	tripartite motif-containing 29	11q22-q23	-3.85555	7e-04	0.989
203431_s_at	RICS	Rho GTPase-activating protein	11q24-q25	-3.85929	9e-04	0.9883
202504_at	TRIM29	tripartite motif-containing 29	11q22-q23	-3.85978	9e-04	0.9882
218484_at	NDUFA4L2	NADH dehydrogenase (ubiquinone) 1 alpha subcomplex, 4-like 2	12q13.3	-3.87078	6e-04	0.9871

Probe ID	Gene Symbol	Description	Cytoband			
208987_s_at	FBXL11	F-box and leucine-rich repeat protein 11	11q13.1	-3.87493	5e-04	0.9868
209885_at	RHOD	ras homolog gene family, member D	11q14.3	-3.9315	9e-04	0.9778
209282_at	PRKD2	protein kinase D2	19q13.3	-3.99405	3e-04	0.9663
212146_at	PLEKHM2	pleckstrin homology domain containing, family M (with RUN domain) member 2	1p36.21	-4.00689	1e-04	0.9638
211452_x_at	LRRFIP1	leucine rich repeat (in FLII) interacting protein 1	2q37.3	-4.01033	3e-04	0.9622
201480_s_at	SUPT5H	suppressor of Ty 5 homolog (S. cerevisiae)	19q13	-4.01411	9e-04	0.9615
222006_at	LETM1	leucine zipper-EF-hand containing transmembrane protein 1	4p16.3	-4.01545	6e-04	0.9609
201851_at	SH3GL1	SH3-domain GRB2-like 1	19p13.3	-4.02886	4e-04	0.9567
218064_s_at	AKAP8L	A kinase (PRKA) anchor protein 8-like	19p13.12	-4.03906	4e-04	0.9538
201396_s_at	SGTA	small glutamine-rich tetratricopeptide repeat (TPR)-containing, alpha	19p13	-4.05052	7e-04	0.9509
210145_at	PLA2G4A	phospholipase A2, group IVA (cytosolic, calcium-dependent)	1q25	-4.07608	6e-04	0.9438
214246_x_at	MINK1	misshapen-like kinase 1 (zebrafish)	17p13.2	-4.0819	2e-04	0.9412
221188_s_at	CIDEB	cell death-inducing DFFA-like effector b	14q12	-4.09479	7e-04	0.9375
201820_at	KRT5	keratin 5 (epidermolysis bullosa simplex, Dowling-Meara/Kobner/Weber-Cockayne types)	12q12-q13	-4.1161	8e-04	0.9306
219186_at	ZBTB7A	zinc finger and BTB domain containing 7A	19p13.3	-4.11726	2e-04	0.9299
205109_s_at	ARHGEF4	Rho guanine nucleotide exchange factor (GEF) 4	2q22	-4.12612	4e-04	0.9268
218749_s_at	SLC24A6	solute carrier family 24 (sodium/potassium/calcium exchanger), member 6	12q24.13	-4.18619	2e-04	0.9007
202424_at	MAP2K2	mitogen-activated protein kinase kinase 2	19p13.3	-4.20348	2e-04	0.893
206491_s_at	NAPA	N-ethylmaleimide-sensitive factor attachment protein, alpha	19q13.32	-4.20557	8e-04	0.8919
203243_s_at	PDLIM5	PDZ and LIM domain 5	4q22	-4.22345	6e-04	0.8828
219476_at	C1orf116	chromosome 1 open reading frame 116	1q32.1	-4.2911	3e-04	0.8451
215714_s_at	SMARCA4	SWI/SNF related, matrix associated, actin dependent regulator of chromatin, subfamily a, member 4	19p13.2	-4.31703	3e-04	0.8302
203239_s_at	CNOT3	CCR4-NOT transcription complex, subunit 3	19q13.4	-4.32181	3e-04	0.8278
211822_s_at	NLRP1	NLR family, pyrin domain containing 1	17p13.2	-4.32779	2e-04	0.8227

Probe	Gene	Description	Cytoband			
219047_s_at	ZNF668	zinc finger protein 668	16p11.2	-4.34226	2e-04	0.8145
203287_at	LAD1	ladinin 1	1q25.1-q32.3	-4.34949	3e-04	0.8087
212280_x_at	ATG4B	ATG4 autophagy related 4 homolog B (S. cerevisiae)	2q37.3	-4.35364	5e-04	0.806
213478_at	KIAA1026	kazrin	1p36.21	-4.3956	5e-04	0.7787
208751_at	NAPA	N-ethylmaleimide-sensitive factor attachment protein, alpha	19q13.32	-4.409	4e-04	0.7701
219278_at	MAP3K6	mitogen-activated protein kinase kinase kinase 6	1p36.11	-4.44387	3e-04	0.7472
216641_s_at	LAD1	ladinin 1	1q25.1-q32.3	-4.4851	4e-04	0.7155
58994_at	CC2D1A	coiled-coil and C2 domain containing 1A	19p13.12	-4.491	3e-04	0.7107
208794_s_at	SMARCA4	SWI/SNF related, matrix associated, actin dependent regulator of chromatin, subfamily a, member 4	19p13.2	-4.53154	3e-04	0.6806
215792_s_at	DNAJC11	DnaJ (Hsp40) homolog, subfamily C, member 11	1p36.31	-4.58501	2e-04	0.6402
212520_s_at	SMARCA4	SWI/SNF related, matrix associated, actin dependent regulator of chromatin, subfamily a, member 4	19p13.2	-4.60619	4e-04	0.6256
210791_s_at	RICS	Rho GTPase-activating protein	11q24-q25	-4.62033	2e-04	0.6135
213766_x_at	GNA11	guanine nucleotide binding protein (G protein), alpha 11 (Gq class)	19p13.3	-4.6531	2e-04	0.5862
203411_s_at	LMNA	lamin A/C	1q21.2-q21.3	-4.65676	1e-04	0.5831
221506_s_at	TNPO2	transportin 2 (importin 3, karyopherin beta 2b)	19p13.13	-4.70998	2e-04	0.5415
221507_at	TNPO2	transportin 2 (importin 3, karyopherin beta 2b)	19p13.13	-4.76858	1e-04	0.4975
211950_at	UBR4	ubiquitin protein ligase E3 component n-recognin 4	1p36.13	-4.79467	1e-04	0.4773
200601_at	ACTN4	actinin, alpha 4	19q13	-5.99771	1e-04	0.0346
217903_at	STRN4	striatin, calmodulin binding protein 4	19q13.2	-6.01986	1e-04	0.033

ANEXO 6: Genes expresados diferencialmente en función de la respuesta a la quimioterapia de inducción (p<0,001)

Probe	Symbol	Description	Cytoband	t-statistic	p-value	adjp
202065_s_at	PPFIA1	protein tyrosine phosphatase, receptor type, f polypeptide (PTPRF), interacting protein (liprin), alpha 1	11q13.3	4.37776	4e-04	0.5335
216903_s_at	CBARA1	calcium binding atopy-related autoantigen 1	10q22.1	3.90132	5e-04	0.9114
211262_at	PCSK6	proprotein convertase subtilisin/kexin type 6	15q26.3	3.68706	3e-04	0.98
212162_at	KIDINS220	kinase D-interacting substrate of 220 kDa	2p24	3.66321	9e-04	0.9838
217921_at	MAN1A2	mannosidase, alpha, class 1A, member 2	1p13	3.26173	9e-04	1
201906_s_at	CTDSPL	CTD (carboxy-terminal domain, RNA polymerase II, polypeptide A) small phosphatase-like	3p21.3	-3.92216	3e-04	0.8979

ANEXO 7: Genes expresados diferencialmente tras comparar los niveles de expresión en los tumores respecto a las mucosas normales (p ajustada < 0,05)

Probe	Symbol	Description	Cytoband	t-statistic	p-value	adjp
219000_s_at	DCC1	defective in sister chromatid cohesion homolog 1 (S. cerevisiae)	8q24.12	15.1934	1e-04	8e-04
206858_s_at	HOXC6	homeobox C6	12q13.3	14.4493	1e-04	0.0017
204475_at	MMP1	matrix metallopeptidase 1 (interstitial collagenase)	11q22.3	13.7019	1e-04	0.0048
210776_x_at	TCF3	transcription factor 3 (E2A immunoglobulin enhancer binding factors E12/E47)	19p13.3	13.3014	1e-04	0.0068
203905_at	PARN	poly(A)-specific ribonuclease (deadenylation nuclease)	16p13	12.1953	1e-04	0.0182
214039_s_at	LAPTM4B	lysosomal associated protein transmembrane 4 beta	8q22.1	12.0178	1e-04	0.021
219493_at	SHCBP1	SHC SH2-domain binding protein 1	16q11.2	12.0057	1e-04	0.021
210511_s_at	INHBA	inhibin, beta A	7p15-p13	11.8133	1e-04	0.0254
213730_x_at	TCF3	transcription factor 3 (E2A immunoglobulin enhancer binding factors E12/E47)	19p13.3	11.7075	1e-04	0.0277
205483_s_at	ISG15	ISG15 ubiquitin-like modifier	1p36.33	11.7012	1e-04	0.0278
218991_at	HEATR6	HEAT repeat containing 6	17q23.1	11.6926	1e-04	0.028
204415_at	IFI6	interferon, alpha-inducible protein 6	1p35	11.6833	1e-04	0.0282
203856_at	VRK1	vaccinia related kinase 1	14q32	11.5896	1e-04	0.0313
208546_x_at	HIST1H2BH	histone cluster 1, H2bh	6p21.3	11.536	1e-04	0.0331
204033_at	TRIP13	thyroid hormone receptor interactor 13	5p15.33	11.4048	1e-04	0.0375
204197_s_at	RUNX3	runt-related transcription factor 3	1p36	11.3576	1e-04	0.0387
213754_s_at	PAIP1	poly(A) binding protein interacting protein 1	5p12	11.2728	1e-04	0.0431
203514_at	MAP3K3	mitogen-activated protein kinase kinase kinase 3	17q23.3	-11.1173	1e-04	0.0499
207935_s_at	KRT13	keratin 13	17q12-q21.2	-11.194	1e-04	0.0467
211465_x_at	FUT6	fucosyltransferase 6 (alpha (1,3) fucosyltransferase)	19p13.3	-11.2168	1e-04	0.0455
210398_x_at	FUT6	fucosyltransferase 6 (alpha (1,3) fucosyltransferase)	19p13.3	-11.2419	1e-04	0.0443
202313_at	PPP2R2A	protein phosphatase 2 (formerly 2A), regulatory subunit B, alpha isoform	8p21.2	-11.2567	1e-04	0.0438
204484_at	PIK3C2B	phosphoinositide-3-kinase, class 2, beta polypeptide	1q32	-11.5077	1e-04	0.0339
213451_x_at	TNXB	tenascin XB	6p21.3	-11.5514	1e-04	0.0323
215288_at	LOC650465	similar to Short transient receptor potential channel 2 (TrpC2)		-11.703	2e-04	0.0278

Probe ID	Gene	Description	Location			
213895_at	EMP1	epithelial membrane protein 1 (mTrp2)	12p12.3	-11.8069	1e-04	0.0255
215800_at	DUOX1	dual oxidase 1	15q15.3	-12.0036	1e-04	0.021
210609_s_at	TP53I3	tumor protein p53 inducible protein 3	2p23.3	-12.021	1e-04	0.0207
208126_s_at	CYP2C18	cytochrome P450, family 2, subfamily C, polypeptide 18	10q24	-12.1425	1e-04	0.0191
209498_at	CEACAM1	carcinoembryonic antigen-related cell adhesion molecule 1 (biliary glycoprotein)	19q13.2	-12.148	1e-04	0.0189
210155_at	MYOC	myocilin, trabecular meshwork inducible glucocorticoid response	1q23-q24	-12.2011	1e-04	0.0182
208116_s_at	MAN1A1	mannosidase, alpha, class 1A, member 1	6q22	-12.2206	1e-04	0.018
211882_x_at	FUT6	fucosyltransferase 6 (alpha (1,3) fucosyltransferase)	19p13.3	-12.2423	1e-04	0.0176
214421_x_at	CYP2C9	cytochrome P450, family 2, subfamily C, polypeptide 9	10q24	-12.2692	1e-04	0.017
212230_at	PPAP2B	phosphatidic acid phosphatase type 2B	1pter-p22.1	-12.2907	1e-04	0.0165
213478_at	KIAA1026	kazrin	1p36.21	-12.2992	1e-04	0.0164
218035_s_at	FLJ20273	RNA-binding protein	4p13-p12	-12.6595	1e-04	0.0116
215103_at	CYP2C18	cytochrome P450, family 2, subfamily C, polypeptide 18	10q24	-12.7557	1e-04	0.0107
203658_at	SLC25A20	solute carrier family 25 (carnitine/acylcarnitine translocase), member 20	3p21.31	-12.9394	1e-04	0.0089
216333_x_at	TNXB	tenascin XB	6p21.3	-12.9589	1e-04	0.0087
220026_at	CLCA4	chloride channel, calcium activated, family member 4	1p31-p22	-13.0307	1e-04	0.0083
214235_at	CYP3A5P2	cytochrome P450, family 3, subfamily A, polypeptide 5 pseudogene 2	7q21.3-q22.1	-13.0555	1e-04	0.0082
213172_at	TTC9	tetratricopeptide repeat domain 9	14q24.2	-13.1891	1e-04	0.0072
209763_at	CHRDL1	chordin-like 1	Xq22.3	-13.7419	1e-04	0.0043
204829_s_at	FOLR2	folate receptor 2 (fetal)	11q13.3-q13.5	-13.7673	1e-04	0.0042
208335_s_at	DARC	Duffy blood group, chemokine receptor	1q21-q22	-13.9506	1e-04	0.0033
209687_at	CXCL12	chemokine (C-X-C motif) ligand 12 (stromal cell-derived factor 1)	10q11.1	-14.0868	1e-04	0.0028
201412_at	LRP10	low density lipoprotein receptor-related protein 10	14q11.2	-14.1849	1e-04	0.0026
217846_at	QARS	glutaminyl-tRNA synthetase	3p21.3-p21.1	-15.1385	1e-04	8e-04
209487_at	RBPMS	RNA binding protein with multiple splicing	8p12-p11	-15.5269	1e-04	6e-04
209488_s_at	RBPMS	RNA binding protein with multiple splicing	8p12-p11	-15.787	1e-04	6e-04

205200_at	**CLEC3B**	C-type lectin domain family 3, member B	3p22-p21.3	-23.0884	1e-04	1e-04
219747_at	**C4orf31**	chromosome 4 open reading frame 31	4q27	-24.1249	1e-04	1e-04

ANEXO 8. Los resultados obtenidos en el estudio de los niveles de expresión de los genes del sistema NHEJ en biopsias pre-tratamiento de pacientes con carcinoma escamoso de cabeza y cuello localmente avanzado tratados con quimioterapia de inducción han sido publicados en la revista "International Journal of Cancer".

"Ku70 predicts response and primary tumor recurrence after therapy in locally advanced head and neck cancer"

Miguel Angel Pavón, Matilde Parreño, Xavier León, Francesc J. Sancho, Maria Virtudes Céspedes, Isolda Casanova, Antonio Lopez-Pousa, Maria Antonia Mangues, Miquel Quer, Agustí Barnadas and Ramón Mangues.

Int J Cancer. 2008 Sep 1;123(5):1068-79.

*Ku*70 predicts response and primary tumor recurrence after therapy in locally advanced head and neck cancer

Miguel Angel Pavón[1], Matilde Parreño[1]*, Xavier León[2], Francesc J. Sancho[3], Maria Virtudes Céspedes[1], Isolda Casanova[1], Antonio Lopez-Pousa[4], Maria Antonia Mangues[5], Miquel Quer[2], Agustí Barnadas[4] and Ramón Mangues[1]*

[1]*Grup d'Oncogènesi i Antitumorals (GOA), Networking Research Center on Bioengineering, Biomaterials and Nanomedicine (CIBER-BBN) and Institut de Recerca, Hospital de la Santa Creu i Sant Pau, Barcelona, Spain*
[2]*Department of Otorhinolaryngology, Hospital de la Santa Creu i Sant Pau, Barcelona, Spain*
[3]*Department of Pathology, Hospital de la Santa Creu i Sant Pau, Barcelona, Spain*
[4]*Department of Medical Oncology, Hospital de la Santa Creu i Sant Pau, Barcelona, Spain*
[5]*Department of Pharmacy, Hospital de la Santa Creu i Sant Pau, Barcelona, Spain*

5-Fluorouracil and cisplatin-based induction chemotherapy (IC) is commonly used to treat locally advanced head and neck squamous cell carcinoma (HNSCC). The role of nonhomologous end joining (NHEJ) genes (*Ku70, Ku80* and *DNA-PKcs*) in double-strand break (DSB) repair, genomic instability and apoptosis suggest a possible impact on tumor response to radiotherapy, 5-fluorouracil or cisplatin, as these agents are direct or indirect inductors of DSBs. We evaluated the relationship between *Ku80, Ku70* or *DNA PKcs* mRNA expression in pretreatment tumor biopsies, and tumor response to IC or local recurrence, in 50 patients with HNSCC. Additionally, in an independent cohort of 75 patients with HNSCC, we evaluated the relationship between tumor Ku70 protein expression and the same clinical outcomes or patient survival. Tumors in the responder group had significantly higher mRNA levels for *Ku70, Ku80* and *DNA-PKcs* than those in the nonresponder group. Ku70 mRNA was the marker most significantly associated with response to IC. Moreover, high tumor Ku70 mRNA expression was associated with significantly longer local recurrence-free survival (LRFS). Ku70 protein expression was also significantly related to response, and patients with higher percentage of tumor cells expressing Ku70 had longer LRFS. In addition, the percentage of Ku70 positive cells, tumor localization and node involvement were significantly associated with overall survival of patient. Therefore, *Ku70* expression is a candidate predictive marker that could distinguish patients who are likely to benefit from chemoradiotherapy or radiotherapy after the induction chemotherapy treatment, suggesting a contribution of the NHEJ system in HNSCC clinical outcome.
© *2008 Wiley-Liss, Inc.*

Key words: Ku70; Ku80; DNA-PKcs; NHEJ; predictive marker; HNSCC; induction chemotherapy

Therapy for locally advanced head and neck squamous cell carcinoma (HNSCC) aims at organ preservation, having displaced radical surgery. Concomitant platinum-based chemoradiotherapy (CRT) has become the standard treatment for this disease.[1] 5-Fluorouracil (5-FU) and cisplatin-based induction chemotherapy (IC), followed by CRT or radiotherapy (RT), has also been used to treat locally advanced HNSCCs, after demonstrating a benefit for organ preservation, loco-regional control and overall survival.[2,3]

Tumor response to IC predicts response to RT and patient survival in locally advanced HNSCC.[4–6] The IC response distinguishes sensitive carcinomas, which will follow a conservative treatment, from nonsensitive carcinomas, which will be treated with surgery. Conservative treatment consists of the administration of CRT (formerly RT alone) aimed at preventing the mutilating effect of surgery.

Despite conventional TNM information having a strong prognostic value in HNSCC,[7] few predictive molecular markers of response to therapy exist in this pathology. Consequently, uncovering predictors of response to IC may improve our ability to anticipate tumor response to subsequent CRT, identifying patients who could benefit from a conservative treatment.

The cytotoxicity of the classic antineoplasic agents (5-FU, cisplatin, radiotherapy) depends of their ability to produce DNA damage in tumor cells. Despite these agents producing different types of DNA damage, all of them directly or indirectly produce DNA double strand breaks (DSB).[8–10] CDDP produces interstrand crosslinks, stops DNA replication and generates DSBs.[11] 5-FU is an analog of uracil that is converted intracellularly to fluorodeoxyuridine monophosphate (FdUMP), a potent inhibitor of the enzyme thymidylate synthetase. This results in a deoxynucleotide (dNTP) pool imbalance, which disrupts DNA replication, generating DSBs.[10] DNA DSB is the most toxic and mutagenic of all DNA lesions. Two mechanisms exist for DSB repair: homologous recombination and nonhomologous end joining (NHEJ). NHEJ has been described as the predominant DSB repair mechanism in mammalian cells.[12]

We hypothesized that the expression of NHEJ DNA repair (*Ku70, Ku80* and *DNA-PKcs*) genes will influence tumor response to therapy on the basis of the following: (*i*) A high frequency of chromosomal translocations and alteration of double strand break (DSB) DNA repair in HNSCCs[13–15]; (*ii*) Direct induction of DSBs by radiation[9] or indirectly by 5-FU[10,16] or cisplatin[8,11]; (*iii*) The major importance of NHEJ in DSB repair, genomic stability maintenance and suppression of translocations in mammalian cells[17,18]; (*iv*) An increased *in vitro* sensitivity to radiation by NHEJ protein inactivation and recovery of resistance by restoration of activity[19–21] and (*v*) Involvement of Ku70, Ku80 and DNA-PKcs in apoptotic signaling after radiation- or chemotherapy-induced DSBs.[22–24]

Patients with locally advanced (Stage III or IV) HNSCC, treated at our institution with induction chemotherapy followed by either CRT/RT or surgery depending on tumor response, participated in a prospective mRNA study ($n = 50$) or in an independent retrospective immunohistochemistry (IHC) study ($n = 75$). We evaluated the relationship between Ku70, Ku80 or DNA-PKcs mRNA, or Ku70 protein expression in pretreatment tumor biopsies, and the degree of tumor response to IC, local recurrence and patient survival. Our aim was to test the capacity of the expression of these genes in identifying patients likely to benefit from a conservative treatment.

Patients and methods

Patient characteristics and treatment plan

Accrual for the mRNA prospective study ($n = 50$) was initiated in 2002. Patients in the IHC retrospective study ($n = 75$) were treated during the 1995–2003 period at the Hospital de la Santa Creu i Sant Pau (HSCSP). All patients had pathologically confirmed, untreated, locally advanced (Stage III or IV) HNSCCs. The HSCSP Ethics Committee approved the study.

In both studies, patients were treated with IC consisting of the administration of cisplatin at a dose of 100 mg/m^2 on day 1, and 5-FU at a dose of 1,000 mg/m^2/day by continuous intravenous infusion on days 2–6 every 3 weeks, per 3 courses. Patients who presented a high tumor response after IC followed a conservative treatment, which consisted of the administration of RT or CRT.

TABLE I – CHARACTERISTICS OF PATIENTS INCLUDED IN THE PROSPECTIVE AND RETROSPECTIVE STUDIES

Patients characteristics	Prospective mRNA study ($n = 50$)	Retrospective IHC study ($n = 75$)
Sex		
Men	45 (90%)	71 (95%)
Women	5 (10%)	4 (5%)
Tumor localization		
Oral cavity	11 (22%)	7 (9.3%)
Oropharynx	7 (14%)	18 (24%)
Hypopharynx	14 (28%)	12 (16%)
Larynx	18 (36%)	38 (51%)
Lynph node involvement		
Present	40 (80%)	41 (55%)
Absent	10 (20%)	34 (45%)
Tumor size (T)		
2	8 (16%)	9 (12%)
3	24 (48%)	50 (67%)
4	18 (36%)	16 (21%)
Histological tumor grade		
Good	5 (10%)	2 (3%)
Moderate	39 (78%)	65 (87%)
Poor	6 (12%)	8 (11%)
Tumor staging (TNM)		
III	12 (24%)	40 (53%)
IV	38 (76%)	35 (47%)
Treatment subsequent to IC		
Radiotherapy	16 (32%)	38 (51%)
Chemoradiotherapy	15 (30%)	4 (5%)
Surgery	19 (38%)	33 (44%)

Patients treated from 1995 to 2002 who presented a high tumor response after IC followed treatment with radiotherapy (RT). CRT was introduced in 2003 as an alternative to RT to treat patients with a substantial IC response. Progressively, CRT displaced RT as the treatment of choice after IC.

RT was administered to the primary tumor and clinically positive nodes in 35 fractions of 2 Gy, each over a 7-week period at a total dose of 70 Gy. Nodal areas not clinically involved by tumor received a total dose of 50 Gy. CRT consisted of RT at the same doses plus 3 cycles of cisplatin at a dose of 100 mg/m^2 on day 1 every 3 weeks.

Patients without significant response to IC were usually treated with surgery followed by RT. The characteristics of patients included in both studies are summarized in Table I.

RNA extraction, cDNA synthesis and quantitative PCR

The prospective study was performed using fresh pretreatment primary tumor biopsies obtained from patients with HNSCC. A sample aliquot was used for pathological diagnosis of the malignancy. Samples with a low content of tumor tissue were excluded from the study. Another aliquot was frozen immediately after taking the biopsy, in cold isopentane (histobath), and placed in liquid nitrogen until RNA processing.

Total RNA was extracted with Trizol® (Invitrogen, Paisley, UK) and the phenol–chloroform method. Samples were then precipitated twice with isopropanol and 70% ethanol, and cleaned-up using RNeasy® Spin columns (Qiagen, Valencia, CA). Total RNA was quantified espectrophotometrically. Reverse transcription was performed using 1.5 µg of total RNA and the High Capacity cDNA Archive Kit (Applied Biosystems, Foster City, CA), in a 50 µL final reaction volume, containing 5 µL of 10× RT buffer, 2 µL of 25× dNTPs mixture, 5 µL of 10× Random Hexamer Primers, 125 U of Multiscribe Reverse transcriptase and 40 U of RNase inhibitor (Invitrogen, Paisley, UK). These mixtures were incubated at 25°C for 20 min, and then at 37°C for 2 hr. Finally, heating at 95°C for 3 min inactivated the reverse transcriptase.

mRNA expression was measured on an ABIPrism 7000 Sequence Detection System (Applied Biosystems, Foster City, CA), using predesigned Taqman® Gene Expression Primer and probe Assays (Applied Biosystems, Foster City, CA), which were available for *Ku70*, *Ku80*, and β-actin (http://www.appliedbiosystems.com). All probes were FAM-labeled, except for β-actin that was VIC-labeled. For *DNA-PKcs* detection, we used Primer Express software v2.0 (Applied Biosystems, Foster City, CA) to design the forward (5′-TGGGAGCATCACTTGCCTTTAATAA-3′) and reverse (5′-CAAACTGTTCCACCAGAGACTCTT-3′) primers and a Taqman® probe (5′-CTTCCCTGAATTCCC-3′) (Table II).

mRNA quantitation was performed, in duplicates, in 20 µL total volume PCR reactions, using 2 µL of each sample cDNA, 10 µL of 2× Universal Taqman Master Mix, 1 µL of primers and probe mixture and 7 µL of H$_2$O, following the manufacturer's recommendations (Applied Biosystems, Foster City, CA). Thermal cycling conditions were 2 min at 50°C, 10 min at 95°C, and 40 cycles at 95°C for 15 s and 60°C for 1 min.

TABLE II – DESCRIPTION OF THE AMPLIFICATION AND HYBRIDIZATION REGIONS FOR mRNA GENE EXPRESSION ANALYSIS BY qPCR IN THE PROSPECTIVE STUDY

Gene	Assay[1]	RefSeq[2]	Interexonic union	Amlicon size (bp)
Ku70	Hs00750856_s1	NM_001469	Exon 1	99
Ku80	Hs00221707_m1	NM_021141	Exon 2/Exon 3	72
DNA-PKcs	–[3]	NM_006904	Exon 27/Exon 28	72
β-actin	Hs99999903_m1	NM_00101	Exon 1	171

[1]Number assigned to predesigned Taqman Gene Expression Assay (Applied Biosystems; http://www.appliedbiosystems.com).–[2]mRNA Reference Sequence amplified using Taqman Gene Expression Assays. Available at the NCBI reference Sequence Database (Refseq).–[3]Custom-made sequence (see Patients and Methods section).

Gene expression results were calculated applying the comparative CT method ($2^{-(\Delta\Delta Ct)}$) as previously described.[25,26] Using the $2^{-(\Delta\Delta Ct)}$ method, the data are presented as the fold change in gene expression normalized to an endogenous gene and relative to a calibration sample. β-actin was used as the endogenous control to normalize the PCR results for the amount of RNA added to the reverse transcription reaction. We extracted RNA from the HNSCC UM-SCC-22A cell line (a gift from Dr. R.H. Brakenhoff), which was used as the calibration sample.[27] First, we subtracted the endogenous gene expression from target gene expression ($\Delta CT = CT_{target\ gene(Ku80,\ Ku70\ or\ DNA-PKcs)} - CT_{endogenous\ gene(\beta-actin)}$) and, afterwards, calculated the expression in the tumor relative to the calibration sample ($\Delta\Delta CT = \Delta CT_{tumor\ sample} - \Delta CT_{calibrator(UM-SCC-22A)}$). Each gene measure was expressed in relation to the level of the same gene in the UM-SCC-22A cell line. This cell line was maintained in 10% FBS DMEM (Invitrogen, Paisley, UK), with 2 mmol/L glutamine, 50U/mL penicillin and 50U/mL streptomycin, at 37°C in a humidified atmosphere containing 5% CO_2.

Immunohistochemistry

We used pretreatment formalin-fixed and paraffin-embedded biopsies of primary HNSCCs, with high tumor tissue content, to perform the retrospective study. Four-micron sections were deparaffinized in xylol and rehydrated using decreasing ethanol concentrations (100, 96, 80, 70 and 50%) and distilled H_2O. The samples were immersed in $1\times$ Target Retrieval Solution pH = 6 (Dako Cytomation S.A., St Just Desvern, Spain) and autoclaved over 10 min at 121°C for antigenic retrieval. Endogenous tissue peroxidase was inactivated by incubating samples in a 3% H_2O_2 solution for 10 min. Samples were then incubated with a mouse monoclonal antibody against Ku70 (Ab-4) (Lab Vision, Freemont, CA) at a 1:200 dilution. For primary antibody detection, we used the EnVision + Dual Link System-HRP Kit in an automatic Autostainer System (DakoCytomation S.A., St Just Desvern, Spain), according to manufacturer's instructions. Counterstaining was performed with hematoxylin (DakoCytomation S.A., St Just Desvern, Spain). Samples were dehydrated in a growing ethanol and xylol gradient, and mounted with DPX media (Sigma Aldrich, Tres Cantos, Spain). Negative controls were processed substituting the primary antibody by nonimmunized mouse serum. A normal mucousa and 2 HNSCC samples were used to control for IHC batch staining variability.

Immunohistochemistry analysis

We took three 100×-magnified images per sample, using a DP50 camera and an Olympus DX51 microscope, under the same lighting and time exposure conditions. The ViewFinder Lite v1.0 and Studio Lite v1.0 software (Olympus, USA) were used to capture and store all images. Afterwards, we eliminated all areas containing no tumor cells, using AdobePhotoshop software v7.0 (AdobePhotoshop systems, USA). We quantitated the IHC staining of the areas containing tumor cells, using the Metamorph v 5.0 (Universal Imaging, Downingtown, PA) software and applied the HSI (HUE-saturation-intensity) model,[28,29] which selects a particular area according to its color, as defined by its HUE (the dominant wavelength of transmitted light), saturation and intensity. For each pixel in an image, the values of HUE, saturation and intensity are independently transformed to one of 256 integral values within a 0–255 range. Setting a range between 0 and 255 for each of these 3 parameters makes it possible the selection of the particular areas of interest.[28,29]

Evaluation of tumor response, local recurrence and patient survival

In both, the prospective and retrospective studies, tumor response was evaluated by comparing tumor volume before IC and after the third cycle of IC. Response was defined as a reduction in primary tumor volume, as measured by physical examination, fiber optic laryngoscopy, and CT scan/MR imaging following RECIST criteria.[30]

The responder group was composed of tumors presenting a complete response or a partial response higher than 50%. The nonresponder group included all tumors presenting a stable disease (<25% progression or <50% reduction) or progressive disease (>25% of progression in tumor volume).

We recorded local recurrence-free survival (LRFS), which was defined as time from diagnosis to recurrence at the primary location of the tumor. In addition, we recorded overall survival, defined as the time from diagnosis to patient death. The median follow-up time in the prospective study was 2.1 years. The median follow-up time for the retrospective study was 4.0 years. The molecular analysis was performed with no knowledge of clinical outcomes.

Statistical analysis

We compared tumor mRNA levels and the percentage of positively stained tumor cells between the responder and nonresponder groups by applying the Mann–Whitney *U* test. We performed a nonparametric receiver-operating characteristics (ROC) analysis to evaluate the diagnostic usefulness of Ku80, Ku70 and DNA-PKcs mRNA levels and Ku70 protein levels to discriminate between responding and nonresponding tumors. We established a cut-off level for mRNA and protein levels for each studied variable to distinguish tumors with high or low expression levels. These cut-off values were determined selecting the most accurate values obtained from the nonparametric ROC analysis, taking into account the best balances between sensitivity and specificity. Logistic regression analysis was used to evaluate the associations of Ku70, Ku80 and DNA-PKcs expression above or below the defined cut-off values, tumor size (T), node involvement and tumor localization, with IC response. Adjusted LRFS curves were estimated using the Kaplan–Meier method. We applied a 2-tailed log-rank test to evaluate the differences in LRFS between patients with tumor expression above or below the defined cut-off values. The association of Ku70, Ku80 and DNA-PKcs gene expression, node involvement, tumor size and localization with LRFS and OS was assessed applying a univariate and a multivariate Cox regression model analysis.

Differences were considered significant at *p* values <0.05 in all applied statistical tests. All statistical analyses were performed using the SPSS software v.14.01 (SPSS, Chicago, IL).

Results

Differences in Ku70, Ku80 and DNA-PKcs mRNA levels between responder and nonresponder tumors (prospective study)

The characteristics of the patients included in the prospective study are summarized in Table I. Twenty-eight out of 50 patients had a tumor response to IC higher than 50% (responder group), whereas 22 tumors showed responses lower than 50% (nonresponder group). The median mRNA level was 4.4 (range 0.5–309.8) for Ku70, 2.3 (0.1–36.8) for Ku80 and 3.3 (0.1–59.9) for DNA-PKcs when considering all samples (responders and nonresponders) included in the prospective study. The median mRNA level in the responder group was 6.6 (range 1.2–236.4) for Ku70, 3.2 (range 0.7–36.8) for Ku80 and 4.2 (range 0.2–59.9) for DNA-PKcs. The median mRNA level in the nonresponder group was 3.3 (range 0.5–309.0) for Ku70, 1.8 (range 0.1–3.3) for Ku80 and 2.4 (range 0.1–11.5) for DNA-PKcs.

We observed significantly higher mRNA tumor values for Ku70 (*p* = 0.005), Ku80 (*p* = 0.002) or DNA-PKcs (*p* = 0.017) in responders than in nonresponders (Figs. 1*a*–1*c*). Afterwards, we performed a ROC analysis to test the sensitivity and specificity of Ku70, Ku80 or DNA-PKcs mRNA levels in evaluating response to IC (Fig. 1*d*). The areas under the curve (AUC) were 0.73 [CI (95%) = 0.59–0.88, *p* = 0.005] for Ku70, 0.76 [CI (95%) = 0.63–0.90, *p* = 0.002] for Ku80 and 0.70 [CI (95%) = 0.55–0.88,
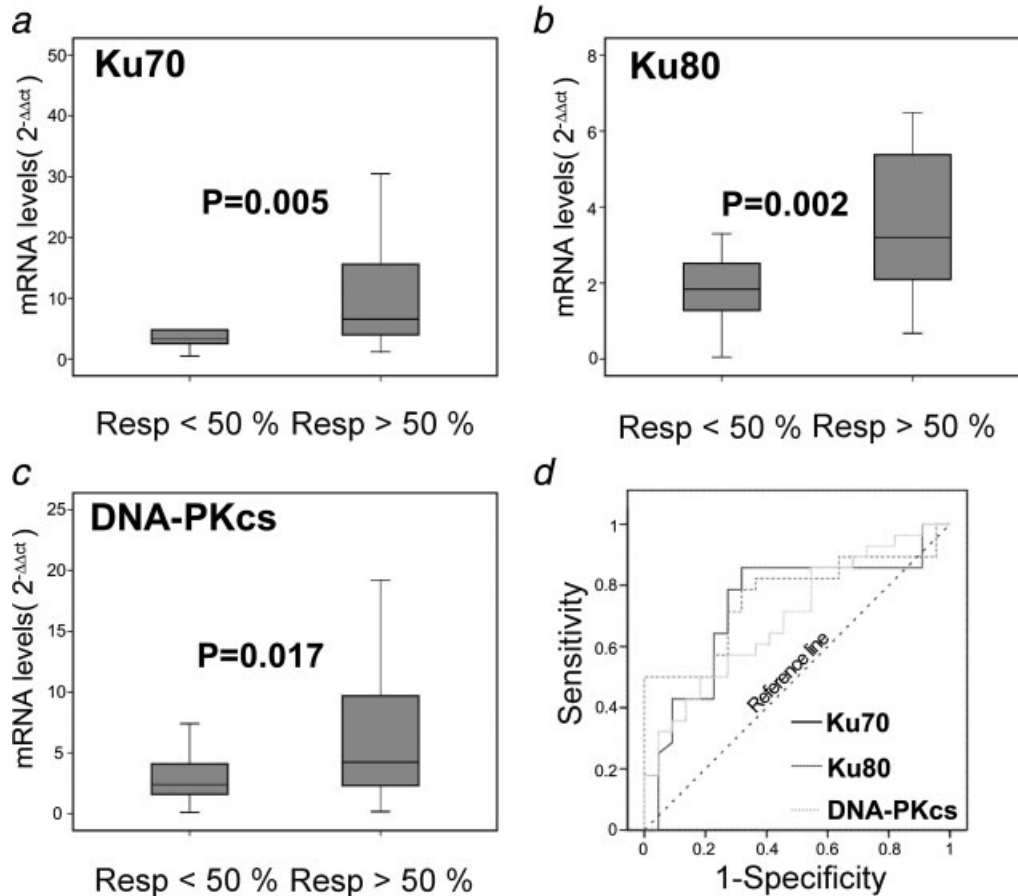
FIGURE 1 – Significant differences in Ku70 (*a*), Ku80 (*b*) and DNA-PKcs (*c*) mRNA levels in pretreatment biopsies between tumors with a response to induction chemotherapy higher than 50% (Resp > 50%) and tumors with response lower than 50% (Resp < 50%) in the prospective study. Differences in NHEJ gene expression between the responder group and the nonresponder group were compared using the nonparametric Mann–Whitney *U* test. (*d*) Curves obtained applying receiver-operating-characteristics (ROC) analysis for Ku70, Ku80 and DNA-PKcs.

$p = 0.017$] for DNA-PKcs. We next established a cut-off level between high and low mRNA levels for each gene by selecting the most accurate value obtained in the ROC analysis. Thus, we distributed all patients between 2 groups, one above and another below the following mRNA thresholds: 3.6 for Ku70, 2.6 for Ku80 and 5.0 for DNA-PKcs. The sensitivity, specificity and accuracy in predicting IC response with the established cut-offs were as follows: Ku70 (sensitivity 86%, specificity 68%, accuracy 78%), Ku80 (sensitivity 57%, specificity 77%, accuracy 66%) and DNA-PKcs (sensitivity 43%, specificity 86%, accuracy 62%).

Logistic regression analysis was conducted to evaluate the associations of mRNA levels, tumor localization, lymph node involvement and tumor size (T) with IC response. Only high (above 3.6) Ku70 mRNA levels were significantly associated with response to IC higher than 50% [$p = 0.03$; odds ratio 5.9; CI (95%) = 1.28–29.6]. Therefore, ROC and logistic regression analysis indicated that Ku70 mRNA gene expression was the best marker to discriminate between responding and nonresponding tumors.

Ku70 and Ku80 mRNA levels are associated with local recurrence-free survival (prospective study)

We next analyzed whether the mRNA expression of these genes was associated with primary tumor recurrence (Fig. 2*a*). Patients whose tumors expressed Ku70 mRNA levels above the established 3.6 threshold had a significantly higher probability of surviving without having primary tumor recurrence (increased LRFS) than patients bearing tumors with lower mRNA levels ($p = 0.043$).

Similarly, patients whose tumors expressed Ku80 mRNA levels above the 2.6 threshold had a higher LRFS than patients bearing tumors with lower mRNA levels ($p = 0.04$). DNA-PKcs mRNA levels did not show an association with patient's LRFS ($p = 0.457$).

We also applied a Cox model analysis to study the association of mRNA levels, tumor size (T), localization, lymph node involvement and IC response, with LRFS (Table III). On a Cox univariate analysis, we found that Ku70 mRNA levels ($p = 0.05$) and Ku80 mRNA levels ($p = 0.05$) were associated with LRFS. On a multivariate Cox analysis, Ku70 mRNA levels ($p = 0.04$) and tumor size ($p = 0.03$) were significant independent risk factors of LRFS. Therefore, in our study, Ku70 gene expression remains the only marker able to consistently predict local control of the disease. Thus, patients with tumors showing high Ku70 mRNA levels presented a higher probability of surviving without primary tumor recurrence than patients with tumors showing low expression of this gene. Ku80 mRNA, despite displaying the same trend as Ku70 and being also a predictive marker of response, showed a weaker association with LRFS.

After applying a Cox model analysis to assess the association of mRNA levels, tumor size (T), localization, lymph node involvement and IC response with overall survival, we observed that high Ku70 levels displayed the same trend towards associating with longer overall survival, as it happened with LRFS; however, the observed differences did not reach statistical significance ($p = 0.14$).
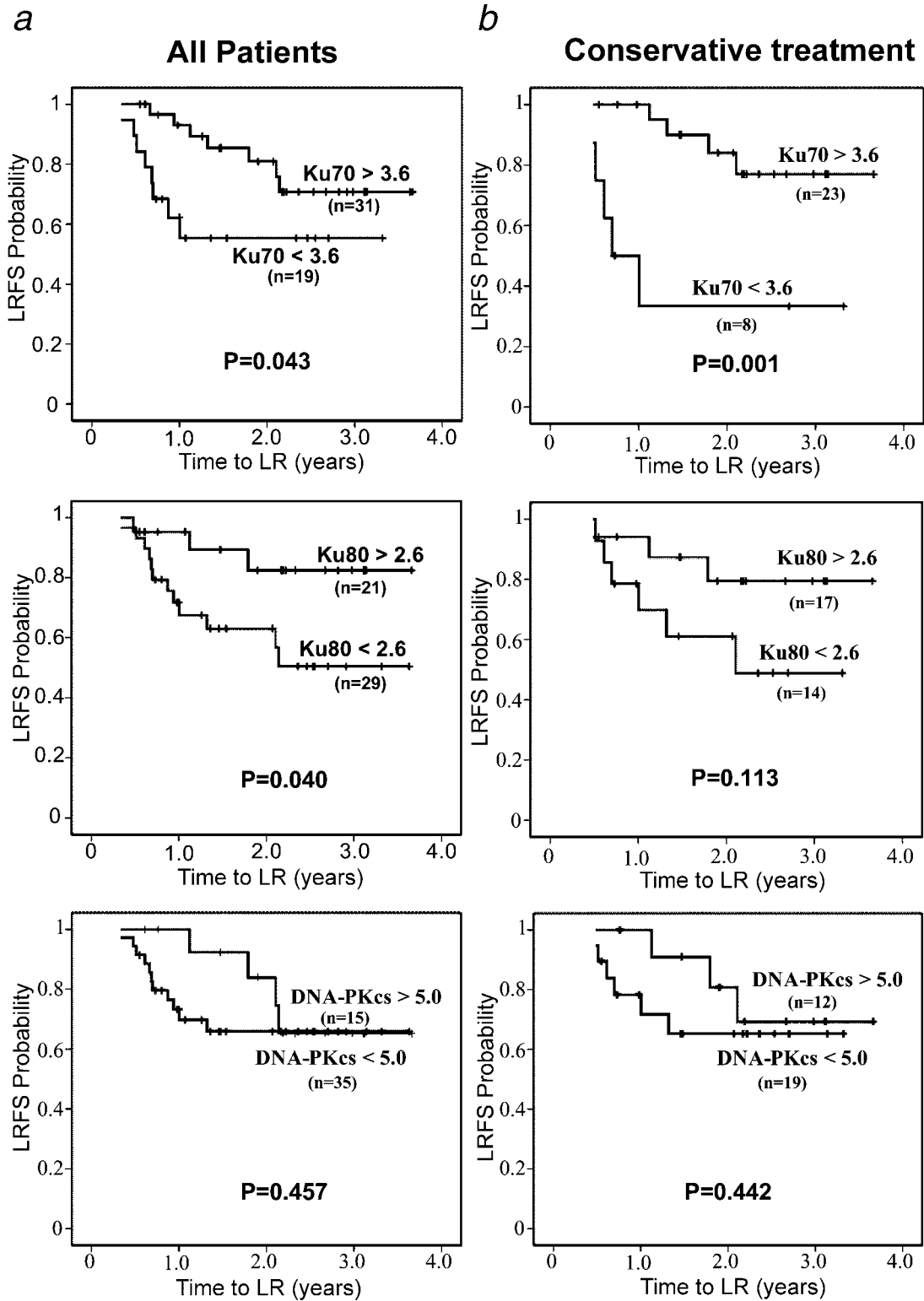
FIGURE 2 – Analysis of patient LRFS in the prospective study. Differences in adjusted local recurrence-free survival (LRFS) between patients bearing tumors expressing pretreatment Ku70, Ku80 or DNA-PKcs mRNA levels above or below the depicted cut-off levels. (*a*) Analysis performed including all patients treated with induction chemotherapy, followed by either surgery or conservative treatment. (*b*) Analysis performed only with the group of patients who followed a conservative treatment after IC.

TABLE III – HAZARD RATIOS FOR LOCAL RECURRENCE OBTAINED APPLYING COX MODEL ANALYSIS IN THE PROSPECTIVE STUDY

	Local recurrence-free survival			
	Univariate		Multivariate	
	HR (95% CI)	*p* value	HR (95% CI)	*p* value
All patients				
KU70 mRNA (<3.6 *vs.* >3.6)	**2.8 (1.0–7.7)**	**0.05**	**4.7 (1.1–19.8)**	**0.04**
KU80 mRNA (<2.6 *vs.* >2.6)	**3.5 (1.0–12.4)**	**0.05**	2.1 (0.5–9.3)	0.34
DNA-PKcs (<5.0 *vs.* >5.0)	1.5 (0.5–4.9)	0.46	1.7 (0.2–12.6)	0.59
Tumor size (T) (T3–T4 *vs.* T1–T2)	2.3 (0.8–6.6)	0.14	**7.4 (1.3–42.9)**	**0.03**
Node involvement (N^+ *vs.* N^0)	2.1 (0.5–9.3)	0.33	1.0 (0.2–6.0)	0.97
Localization	1.4 (0.4–4.3)	0.60	2.1 (0.5–8.6)	0.32
Conservative treatment				
Ku70 mRNA (<3.6 *vs.* >3.6)	**6.9 (1.9–26.5)**	**<0.01**	**28.2 (1.7–47.0)**	**0.02**
Ku80 mRNA (<2.6 *vs.* >2.6)	2.9 (0.7–11.8)	0.13	0.9 (0.0–8.6)	0.95
DNA-PKcs (<5.0 *vs.* >5.0)	1.7 (0.4–6.9)	0.45	0.4 (0.02–7.3)	0.53
Tumor size(T) (T3–T4 *vs.* T1–T2)	1.8 (0.4–7.2)	0.42	4.9 (0.7–36.1)	0.12
Node involvement (N^+ *vs.* N^0)	2.6 (0.3–20.6)	0.37	1.3 (0.1–16.5)	0.85
Localization	1.1 (0.2–5.1)	0.94	0.5 (0.1–3.2)	0.45

The bold values indicate the existence of statistically significant differences.

Ku70 mRNA levels are associated with local recurrence-free survival in patients who followed a conservative treatment (prospective study)

We next searched for the possible differences in adjusted LRFS within the subset of patients who received CRT or RT after IC (*n* = 31), excluding those treated with surgery after IC (*n* = 19) (Fig. 2b). Our objective was to study Ku70, Ku80 and DNA-PKcs as possible markers of tumor response and primary tumor recurrence after genotoxic therapy. Surgery is applied to patients with poor response to IC, and their inclusion could have altered the LRFS registered in patients under genotoxic treatment. All patients (*n* = 28) of the responder group followed a treatment with CRT or RT after IC. Nineteen patients of the nonresponder group underwent surgical excision of their tumors after IC. Three patients of the nonresponder group refused mutilating surgery and, contrarily to medical advice, were treated with RT or CRT. Out of the 31 IC patients who followed a conservative treatment (CRT or RT) after IC, those whose tumors expressed Ku70 mRNA levels above the 3.6 threshold had a significantly higher probability of surviving without having a primary tumor recurrence (increases LRFS) than patients bearing tumors with lower mRNA levels (*p* = 0.001). Moreover, patients whose tumors expressed Ku80 mRNA levels above the 2.6 threshold showed a trend towards increased LRFS, but it did not reach statistical significance (*p* = 0.113). DNA-PKcs mRNA levels did not show significant differences in patient's LRFS (*p* = 0.442).

A univariate Cox model analysis confirmed the significant association between Ku70 mRNA levels and LRFS (*p* < 0.01) (Table III). Moreover, a multivariate Cox model analysis showed that Ku70 mRNA was the only independent risk factor for local recurrence-free survival in patients who followed conservative treatment after IC (*p* = 0.02) (Table III).

On a multivariate analysis, the difference in relative risk of primary tumor recurrence between high and low Ku70 mRNA tumor patients was 6 times higher when only conservatively treated patients were included in the analysis than when all patients were included (HR: 28.2 *vs.* 4.7, Table III). A univariate (*p* = 0.23) and a multivariate (*p* = 0.64) Cox model analysis in patients treated with surgery after IC showed no association between Ku70 mRNA levels and LRFS. The capacity of Ku70 mRNA in predicting local recurrence after conservative treatment was improved when the data on LRFS after mutilating surgery were excluded from the analysis, indicating that Ku70 mRNA is a better marker of local recurrence after CRT/RT than of recurrence after surgery.

Differences in Ku70 protein expression between responder and nonresponder tumors (retrospective study)

Patient characteristics in the retrospective study are summarized in Table I. Out of 75 analyzed patients, 39 had a tumor response to

IC greater than 50% (responder group), whereas 36 patients showed a tumor response lower than 50% (nonresponder group). Ku70 immunohistochemical analysis showed an exclusively nuclear staining pattern. Using the "Set color threshold" tool of Metamorph v5.0 software and the HSI color model (Fig. 3a), we established a 180–255 HUE range to select all brown primary antibody-stained areas (positive nuclei) (Fig. 3c), which ensured the absence of any selected area in negative control samples. Moreover, we established a 160–255 HUE range to select all (brown + blue) tumor cell nuclei present in the sample (Fig. 3d), leaving out cell cytoplasm, membrane or keratin deposits. Since all tumor nuclei present in each sample image displayed a similar size, we calculated the percentage of positive tumor cells dividing the area occupied by positive tumor nuclei by the area occupied by all nuclei. Two experienced pathologists validated this method.

Figure 4a shows Ku70 staining in 2 tumors from patients with different responses to IC treatment. The median of the percentage of Ku70 positively stained cells was 63.31 (range 7.4–92.8) for all samples (responders and nonresponders) included in the retrospective study. The median of the percentage of Ku70 positively stained cells in the responder group was 70.7% (range 19.0–92.8%) and in the nonresponder group was 57.7% (range 7.4–88.3%). We observed a significantly higher percentage of Ku70 positive tumor cells in responders than in nonresponders (*p* = 0.036) (Fig. 4b). Using ROC analysis, we obtained an AUC of 0.64 [CI (95%) = 0.51–0.77, *p* = 0.036] for Ku70 positive cells (Fig. 4c). The cut-off value between high and low percentage of positive Ku70 cells was established at 74%, which was the most accurate value obtained in the ROC analysis. Its sensitivity, specificity and accuracy in predicting IC response was 47, 69 and 59%, respectively. Thus, in pretreatment tumor samples, the percentage of Ku70 positive tumor cells was significantly associated with response to IC.

Association between the percentage of Ku70 positive cells and local recurrence-free survival (retrospective study)

Patients whose tumors contained a percentage of Ku70 positive cells above the 74% threshold had a significantly increased probability of surviving without having a primary tumor recurrence (longer LRFS), as compared to patients whose percentage of positive tumor cells were below this threshold (*p* = 0.013) (Fig. 4d). Cox univariate (*p* = 0.03) and multivariate (*p* = 0.02) analyses revealed the percentage of Ku70 positive tumor cells as the most significant factor associated with LRFS (Table IV).

Similar to the mRNA prospective study, in this study, we analyzed the adjusted LRFS within the subset of patients who received RT or CRT after IC, excluding patients who underwent a surgery procedure after IC. All patients (*n* = 39) of the responder group followed a treatment with CRT or RT after IC. Thirty-three
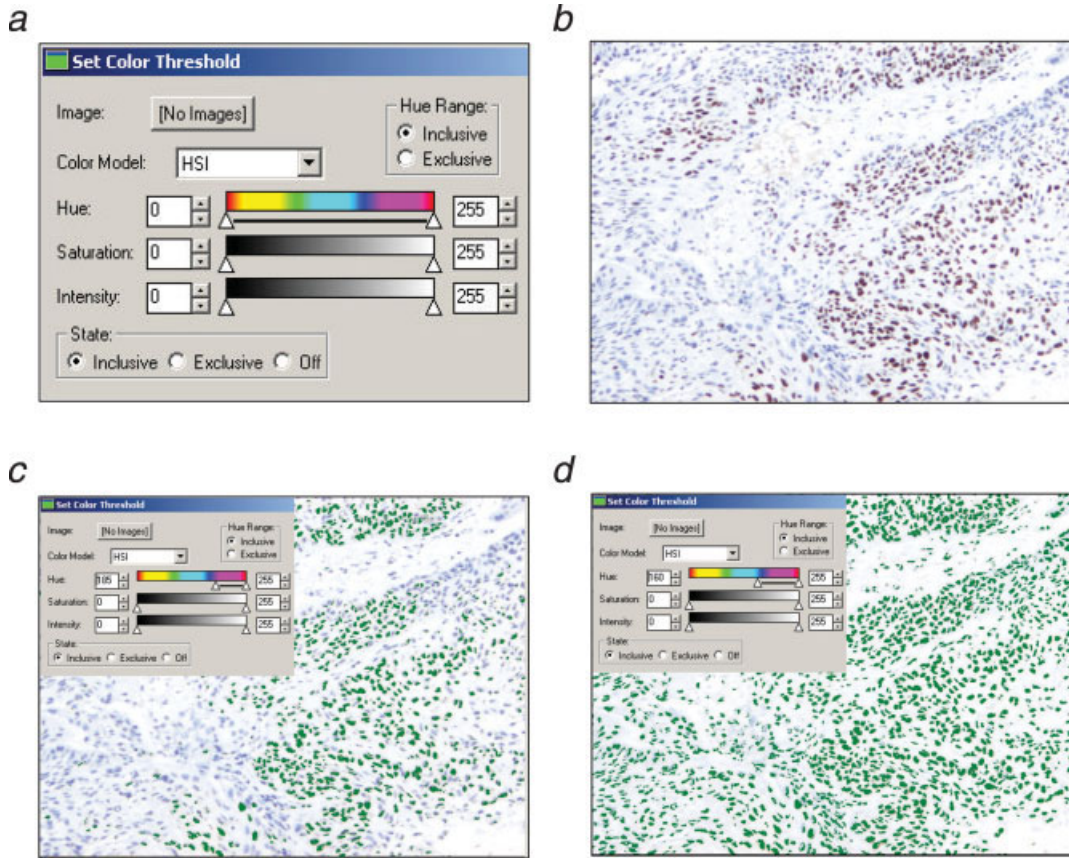
FIGURE 3 – Ku70 Immunohistochemistry quantification used in the retrospective study. (*a*) We used the "Set Color Threshold" tool, implemented in Metamorph software v5.0, to establish a suitable HUE range that selects areas presenting specific immunostaining characteristics. (*b*) Immunohistochemistry quantification was performed in 100× magnified images. Ku70 shows a nuclear staining pattern. (*c*) All positive immunostained nuclei, present in the image, were selected using a 180–255 HUE range (green areas). (*d*) All the nuclei (positive and negative), present in the image, were selected using a 165–255 HUE range (green areas).

patients of the nonresponder group followed a surgery treatment after IC. Three patients of the nonresponder group, contrarily to medical advice, rejected mutilating surgery and followed CRT or RT treatment. A total of forty-two patients followed a conservative treatment after IC. Patients whose tumors contained a percentage of Ku70 positive nuclei above the established 74% threshold had a significantly longer LRFS as compared to patients whose percentage of positive tumor nuclei were below this threshold ($p = 0.008$) (Fig. 4*e*). Cox univariate ($p = 0.03$) and multivariate ($p = 0.02$) analyses confirmed the association between the percentage of Ku70 positive tumor cells and LRFS in patients who followed conservative treatment after IC (Table IV). A univariate ($p = 0.51$) and a multivariate ($p = 0.48$) Cox model analyses in patients treated with surgery after IC showed no association between the percentage of Ku70 positive tumor cells and LRFS.

In summary, high percentage of Ku70 positive cells was significantly associated with a longer local primary-recurrence-free survival. In addition, the predictive capacity of Ku70 protein expression became more significant when analyzing only patients under conservative treatment than when including all patients (conservative plus surgical) in the analysis (see Figs. 4*d* and 4*e*).

*Association between the percentage of Ku70 positive cells and overall survival (retrospective study)*

On a Cox univariate analysis, we found that the percentage of tumor Ku70 positive cells ($p = 0.03$), node involvement ($p = 0.03$) and tumor localization ($p < 0.01$) were significantly associated with patient's overall survival (Table IV). Moreover, on a multivariate Cox analysis, only the percentage of Ku70 positive

cells ($p < 0.01$) and tumor localization ($p < 0.01$) were significant independent risk factors of overall survival (Table IV). Performance of the same analysis only on patients who underwent conservative treatment after IC yielded similar results (Table IV).

Discussion

The aim of this work was to obtain predictive markers of response to therapy in locally advanced HNSCCs. In the prospective study, we have described that tumors showing a response higher than 50% to induction chemotherapy (IC) had significantly higher pretreatment Ku70, Ku80 or DNA-PKcs mRNA levels than tumors with a response lower than 50%. In the retrospective study, which was carried out in a distinct cohort of patients, we analyzed Ku70 tumor expression, because it was the best marker of response and local recurrence in the prospective analysis. This study included a higher number of patients and longer follow-up times allowing to perform a more extensive local recurrence and overall survival analysis. Here, our goal was to know if the observed relationship between Ku70 expression and the clinical variables described in the prospective study was also found in the retrospective study and whether these findings went in the same direction, despite using a different methodology (IHC instead of qPCR).

In the retrospective study, *Ku70* was the most significant independent factor in predicting LRFS, being also associated with OS. In contrast, node involvement and tumor localization were associated with overall survival, but they did not predict LRFS. The observed differences between the LRFS and OS analyses suggest
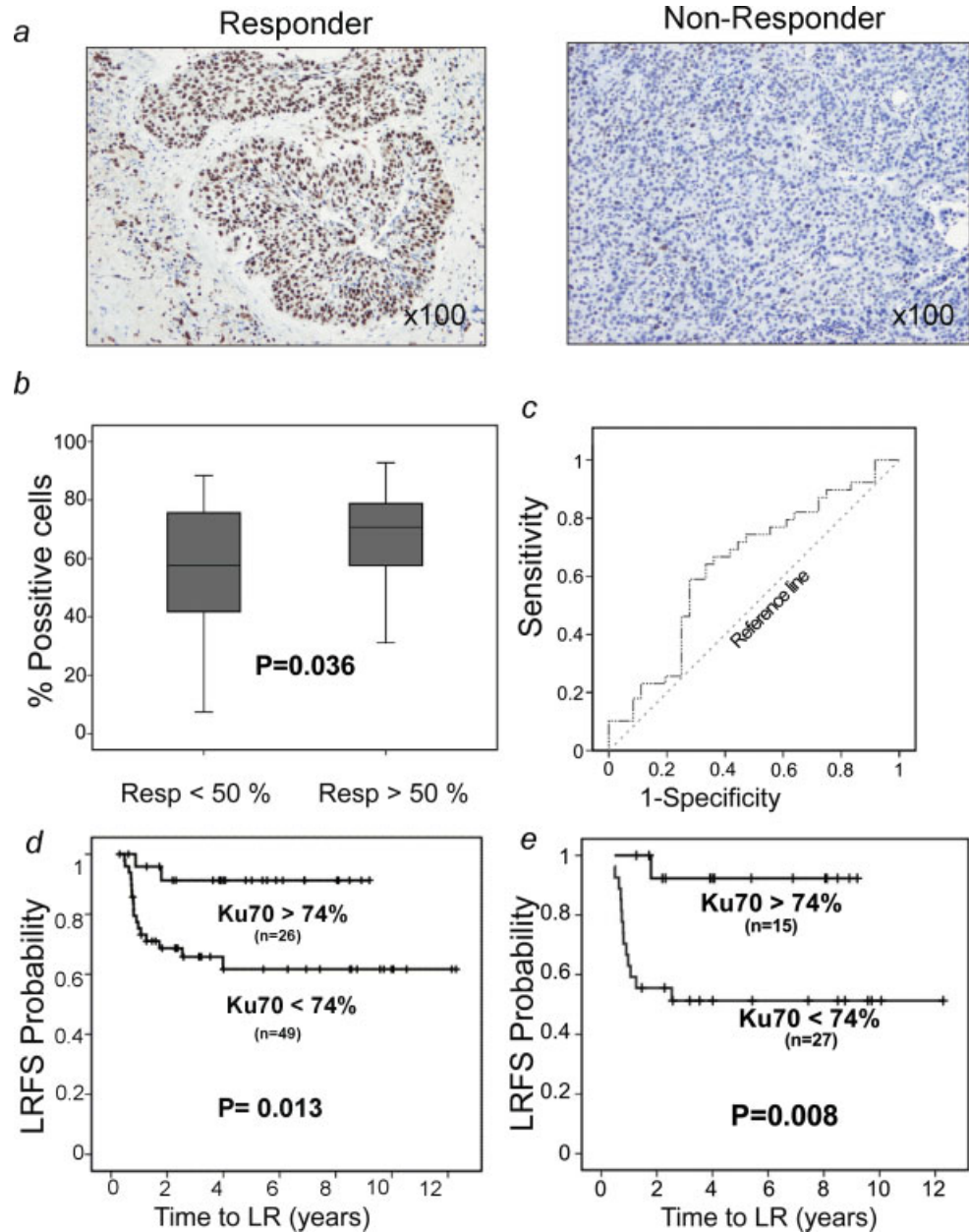
FIGURE 4 – Analysis of Ku70 protein expression in the retrospective study. (*a*) Differences in Ku70 immunostaining in pretreatment biopsies between a representative tumor in the responder group and a representative tumor in the nonresponder group. (*b*) Significant differences in the percentage of Ku70 positive tumor cells between tumors with a response to induction chemotherapy higher than 50% (Resp >50%) and tumors with response lower than 50% (Resp <50%). (*c*) Receiver-operating-characteristics (ROC) curves applied to the percentage of Ku70 positive cells. (*d, e*) Differences in adjusted local recurrence-free survival (LRFS) between patients bearing tumors with a percentage of Ku70 protein staining higher or lower than 74%. (*d*) Analysis performed including all patients treated with induction chemotherapy, followed by either surgery or conservative treatment. (*e*) Analysis performed only in the group of patients who followed a conservative treatment after IC.

that clinical factors other than primary tumor recurrence are involved in determining overall survival. Indeed, node involvement and distant metastases, together with primary tumor recurrence, are the factors showing the highest association with poor prognosis in patients with HNSCC.[7,31]

These results support the notion that *Ku70* expression is a predictive marker of response and recurrence after adjuvant therapy. In this sense, it differs from classical prognostic factors such as tumor localization or node involvement, which associate with clinical outcomes independently of the applied treatment. Thus, prognostic markers are related to tumor aggressiveness and to the nature of the mutations driving cell growth, motility and dissemination capacity, which may not necessarily relate to tumor response to therapy. In contrast, predictive markers are related to the interaction between the tumor and the therapeutic agents and anticipate tumor response. In HNSCC, prognosis largely depends on conventional TNM information, which stratifies patients in terms of tumor aggressiveness, and indicates the requirement or not for systemic therapy. However, this information has so far proven inadequate in predicting response to nonsurgical therapy.[7,32] Thus, despite lymph node involvement is the single most adverse independent prognostic factor[31]; it is, however, not useful in predicting response to adjuvant therapy.[32]

Our finding of Ku70 gene or protein expression as a marker of tumor response to IC, as well as a marker of local disease control and patient survival after genotoxic therapy, suggest that this protein contributes to determine tumor response. These associations are consistent with the previous demonstration that tumor response to IC predicts response to subsequent RT[4,33] and patient survival.[5] To our knowledge, no previous report has addressed the prediction of response to therapy by NHEJ genes/proteins in patient biopsies of locally advanced head and neck squamous cell carcinoma (HNSCC) treated with chemoradiotherapy. We are aware of only 2 related studies, 1 performed in primary cultures from mostly Stage IV head and neck carcinoma biopsies, which found no correlation between DNA-PKcs protein levels and *in vitro* radiosensitivity.[34] Another study evaluated DNA-PKcs, Ku70 and Ku80 expression in head and neck cancer patients treated with radiotherapy

TABLE IV – HAZARD RATIOS FOR LOCAL RECURRENCE AND CANCER DEATH OBTAINED APPLYING COX MODEL ANALYSIS IN THE RETROSPECTIVE STUDY

| | Local recurrence-free survival | | | | Overall survival | | | |
| | Univariate | | Multivariate | | Univariate | | Multivariate | |
	HR (95% CI)	p value	HR (95% CI)	p value	HR (95% CI)	p value	HR (95% CI)	p value
All patients								
%Ku70 positive cells (<74% vs. >74%)	**5.2 (1.2–22.9)**	**0.03**	**5.6 (1.3–24.3)**	**0.02**	**3.9 (1.2–13.3)**	**0.03**	**5.1 (1.5–17.4)**	**<0.01**
Tumor size (T) (T3–T4 vs. T1–T2)	2.7 (0.4–20.1)	0.34	2.7 (0.4–21.4)	0.34	1.4 (0.3–6.0)	0.65	2.2 (0.5–9.6)	0.30
Node involvement (N$^+$ vs. N^0)	1.1 (0.5–2.8)	0.78	1.0 (0.4–3.0)	0.97	**3.1 (1.1–8.3)**	**0.03**	1.9 (0.6–5.8)	0.26
Localization	1.9 (0.8–4.9)	0.17	2.3 (0.8–6.7)	0.12	**5.9 (2.0–17.4)**	**<0.01**	**5.6 (1.7–18.4)**	**<0.01**
Conservative treatment								
%Ku70 positive cells (<74% vs. >74%)	**9.5 (1.3–73.1)**	**0.03**	**12.3 (1.6–96.6)**	**0.02**	2.0 (0.7–13.9)	0.16	**5.5 (1.1–26.5)**	**0.03**
Tumor size (T) (T3–T4 vs. T1–T2)	3.3 (0.4–25.0)	0.26	4.6 (0.6–38.2)	0.16	2.4 (0.3–18.4)	0.42	5.6 (0.7–46.9)	0.11
Node involvement (N$^+$ vs. N^0)	1.0 (0.4–2.9)	0.99	1.7 (0.5–5.2)	0.37	2.2 (0.6–8.1)	0.26	2.5 (0.6–10.2)	0.19
Localization	2.0 (0.7–6.0)	0.22	**2.8 (0.9–9.0)**	**0.08**	**12.3 (1.6–96.6)**	**0.02**	**16.4 (2.0–134.3)**	**<0.01**

The bold values indicate the existence of statistically significant differences.

and found no relationship with radiosensitivity.[35] Nevertheless, there are some clinical reports regarding NHEJ protein prediction of response to therapy on related tumor types. Thus, in agreement with our results, high expression of DNA-PKcs, detected by immunohistochemistry, is associated with response to chemoradiation in esophageal carcinomas.[36] Similarly, high expression of Ku80 or DNA-PKcs protein associates with increased survival in tonsillar carcinoma patients treated with radiotherapy.[37] In contrast to these and to our results, high levels of Ku70 or DNA-PKcs, measured by IHC, associate with lower locoregional control after concurrent chemoradiotherapy in patients with nasopharyngeal carcinoma[38]; nevertheless, this is considered a tumor entity different from HNSCCs.[39] In addition, results predicting response by Ku70 and/or Ku80 proteins by IHC, in a direction opposed to our findings, are also found in other tumor types such as cervical carcinoma, since high levels of these proteins associate with lower response and survival to radiotherapy in patients with cervical cancer.[40,41]

Cell type-dependent response to therapy involving NHEJ proteins

Despite our identification of Ku70 and, to a lesser degree, Ku80 or DNA-PKcs as possible predictive markers of response to CRT in HNSCC, our findings went in a direction contrary to that anticipated. We were expecting higher NHEJ protein levels, or increased DNA-PK complex activity, being related to enhanced DNA damage repair, which in turn would lead to lower tumor responses to therapy. This assumption is based on previous *in vitro* and clinical reports involving DNA repair proteins. For instance, *in vitro* inactivation of NHEJ proteins associates with higher radiosensitivity, whereas restoration of repair activity restores resistance.[21] Moreover, high Ercc1 levels predict for poor response in nonsmall cell lung[42] or ovarian[43] carcinoma patients.

Searching for a possible mechanistic explanation of the unanticipated direction of our findings, we have exhaustively reviewed the *in vitro* and *in vivo* literature that evaluates the role of NHEJ proteins in response to DNA damage. Despite recognizing inconsistency of our results with some previous work, we also found solid work agreeing with our findings. Overall, the literature reports that response to genotoxic therapy by DNA repair proteins depends on the studied cell type,[44] on its differentiation state[45] or even on its degree of functional activation.[46] In the following, we are describing findings, in specific cell types, in which inactivation, or low level of activity, of the NHEJ system decreases their sensitivity to genotoxic agents, and its possible mechanistic basis. Afterwards, we are describing results in other cell types, in which inactivation of NHEJ proteins leads to increased cell sensitivity.

In agreement with the direction of our findings, inactivation of Ku70, in the chicken B lymphocyte cell line DT40, significantly increases their viability when exposed to high doses of double strand break (DSB) inducers, such as γ-radiation or methyl methanesulfonate, as compared with wild type cells.[47] Similarly, enhanced cell survival, through suppression of p53-dependent apoptosis, has been reported in thymocytes of DNA-PKcs−/− mice treated with whole body-ionizing radiation, as compared to wild type mice.[48] In addition, DNA damage-induced apoptosis by ionizing γ-radiation is abolished in DNA-PKcs−/− mouse embryo fibroblasts (MEFs) expressing E1A.[49] Moreover, cisplatin induces marked cell death in Ku80+/+ immortalized MEFs, Ku80+/+ Chinese hamster ovary-derived (CHO) cells or SCID cells complemented with human DNA-PK, as compared with their matched deficient counterparts. This cisplatin induced-death is mediated by the kinase function of the DNA-PK complex and conveyed to neighboring cells through gap junctions, whereas cells deficient in Ku80 or DNA-PKcs are markedly resistant to the drug.[24] In agreement with a role for the DNA-PK complex proteins in apoptosis, the exposure of MEFs or glioma cell lines to γ-radiation leads to DNA-PK and Chk2 phosphorylation of p53, which mediates subsequent induction of apoptosis.[50,51] Similarly, the apoptosis

induced by IGFBP-3 in glioblastoma or prostate cancer cell lines is blocked when DNA-PK is knocked out or chemically inhibited.[52] In addition, in breast cancer cells exposed to ionizing radiation, a nuclear trimeric protein complex, including clusterin, Ku70 and Ku80, is formed that constitutes a death signal for severely damaged cells.[53]

In contrast to the results described above, the role of the NHEJ proteins in DNA repair is consistent with the association between low Ku70 expression or DNA-PK activity and sensitization to radiation in fourteen esophageal cancer cell lines.[54] Similarly, downregulation of Ku70 or DNA-PKcs by siRNA induces sensitization to cisplatin, etoposide or topotecan in the human cervical carcinoma HeLa cell line.[20] Also, in low-passage normal human fibroblasts, siRNA knockdown of DNA-PKcs resulted in increased radiosensitivity.[19] Moreover, enhanced NHEJ DNA repair activity is associated with lower sensitivity to genotoxic agents in primary cultures of human B-chronic lymphocytic leukemia cells, so that treatment with DNA-PK inhibitors increases their sensitivity to the DSB inducers γ-radiation, etoposide or neocarzinostatin.[55] Similarly, Ku70−/− embryonic stem cells have showed an increased sensitivity to γ-radiation as compared to Ku70 heterozygous or wild type embryonic stem cells.[56] These findings suggest that NHEJ proteins may function in DNA repair.[46,57] Moreover, DNA-PKcs may also participate in a NFkB-dependent antiapoptotic pathway that protects cells from death induced by toposisomerase inhibitors, in SV40-transformed human fibroblasts or CHO cells or p53 null MEFs.[58] Similarly, DNA-PKcs inhibits apoptosis induced by heat shock treatment in HeLa, CHO or mouse lung fibroblast cells, a distinct function from its involvement in DNA repair.[59]

Therefore, the apparent contradiction between the results supporting and opposing our findings is solved when considering the existence of a cell type-dependent response to genotoxic therapy. Consistent with this notion, response to DNA damage by double strand break (DSB) inducers, involving the NHEJ system, is cell type-dependent.[46] Thus, a cell type-dependent response to DNA damage, mechanistically involving the DNA-PK complex, has been proposed on the basis of 2 main and alternate functions. The activation of the DNA-PK complex by radiation or other genotoxic agents could trigger signaling pathways that result in apoptosis or cell cycle arrest.[44] Cells, whose physiological function involves their rapid proliferation (*e.g.*, lymphocytes), may require active apoptotic pathways to avoid tumorogenesis after genotoxic damage; in contrast, cells playing a supportive role to other cell types (*e.g.*, stroma providing growth factors to epithelial cells) may instead enter senescence, to maintain their function while avoiding transformation.[44] In agreement with the described cell type dependency, cells with the same genetic background, but at distinct differentiation states, respond differently to genotoxic agents, in the same mouse model. Thus, DNA-PKcs−/− embryonic stem (ES) cells show a similar level of sensitivity to IR than wild type ES, whereas DNA PK−/− fibroblasts (differentiated) cell line derived from the same mice are significantly more sensitive to IR than its wild type counterpart.[45] On the other hand, some cell types change the NHEJ protein function, as they change their activation status. Thus, in nonactivated human multiple myeloma (MM) cells, Ku80 confers sensitivity to DNA damage; however, CD40 activation of MM cells induce Ku80 and Ku70 translocation to the plasma membrane changing their function towards antiapoptosis, which then leads to protection against apoptosis triggered by irradiation or doxorubicin.[60]

Further support for a cell type-dependent role of NHEJ in response to genotoxic therapy comes from findings in some cell types, in which the DNA complex does not appear to play any role in determining response to genotoxic agents. Thus, the sensitivity to IR in mouse ES cells knock out for Artemis, a member of the NHEJ pathway, does not vary as compared to ES wild type cells.[61] Similarly, DNA-PK-deficient murine SCID embryogenic fibroblast or the DNA-PKcs−/− human glioma cell line MO59J shows a similar sensitivity to etoposide as wild type MEFs or the DNA-PKcs+/+ MO59K glioma cell line.[62] Moreover, in human lym-

phoblastic cell lines, siRNA knockdown of DNA-PKcs results in no significant increase in radiosensitivity.[19]

We also reviewed whether other proteins involved in DNA repair followed a cell type-dependent response to genotoxic agents. We choose to focus on p53 role, because it is the most extensively studied gene regarding response to chemotherapy and/or radiotherapy, and because of its involvement in processes similar to those of the NHEJ proteins (DNA repair, apoptosis, genomic stability) and of its functional link with NHEJ signaling.[48–50] We observed a pattern of response to DNA damage similar to that described above for the NHEJ system. Thus, p53 mutation may be a predictive marker of response to 5-FU and cisplatin-based neoadjuvant chemotherapy in HNSCC patients, since tumors with no response have a significantly higher prevalence of p53 mutations than responder tumors.[63] Moreover, we also found a clear cell-type-dependent pattern of response to genotoxic agents in tumors other than HNSCC, as a function of their p53 status. Thus, inactivation of p53 shows either sensitivity or resistance to DNA damage depending on the tumor type, cancer cell line or primary cell line being tested.[57] Tumors bearing a p53 wild type gene show higher response to radiotherapy/chemotherapy, which associates with longer patient survival, while its mutational inactivation leads to lower response and survival in nonsmall cell lung,[64] breast[65] or ovarian[66] carcinoma. In contrast to these results, an increased response in p53 mutant testicular,[67] glioma[68] or bladder[69] tumors has been observed, as compared to p53 wild type tumors.[67] Moreover, and similar to NHEJ proteins, p53 functions in DNA repair as well as in apoptotic regulation,[57] which could lead to contrary outcomes regarding response to genotoxic therapy. Therefore, some of the p53 results that have been reported could be unexpected if only the participation of p53 in DNA repair was considered rather than acknowledging a complex and cell-dependent role in DNA repair and apoptosis.

Overall, the literature reports that cell response to genotoxic therapy in human tumors, or in *in vitro* and *in vivo* models, after the inactivation of NHEJ proteins (and also of p53) depends on the studied cell type, and or its differentiation state or functional activation. These studies demonstrate the increasing complexity of this area of research; thus, in addition to its function in DNA repair and stress response, the proteins of the DNA-PK complex (DNA-PKcs, Ku70 and Ku80) are implicated in multiple and/or separated pathways that regulate distinct cell death pathways.

In summary, our results in HNSCCs could be explained considering that, in addition to their expected DNA repair function, the NHEJ proteins participate in cell apoptotic regulation. Thus, in a particular cell type (*e.g.*, head and neck carcinoma), higher levels of each of these proteins could enhance apoptosis (signaling through the pathways available for this cell type, considering that they remain active after transformation) and lead to a higher tumor response. In contrast, in other cell types, in which apoptotic pathways are blocked, or in which NHEJ proteins participate only in repair functions, higher levels of these proteins would lead to increased repair and lower tumor responses. Therefore, the crosstalk between the available repair and apoptotic functions of the specific repair system (*e.g.*, NHEJ) in a specific cell type (*e.g.*, HNSCC) could determine if the treated cell is sensitive or resistant to the damaging agent (*e.g.*, DSB inducer). Nevertheless, the complexity of this area requires the mechanistic dissection of the candidate pathways, as they relate to our results, before we could establish a definite role for some of the NHEJ proteins in HNSCC cells. We are now starting to address this issue.

Clinical implications of our findings

Independent of the exact role that *Ku70* gene plays, our results support its use as a predictor of response to therapy, primary tumor recurrence and patient survival. Moreover, our results need to be validated in independent studies before their clinical introduction, as it should happen with other proposed markers (*e.g.*, *p53* or HPV infection), which are not still in use.[63,70,71] Finally, in an attempt to extend their possible predictive capacity, we are now

evaluating whether NHEJ genes may also predict HNSCC response to primary concomitant CRT.

In summary, our results suggest that Ku70 mRNA could be a good candidate to be validated as a predictive marker of response to genotoxic therapy. Thus, in biopsies of locally advanced HNSCCs, the levels of tumor mRNA or the percentage of protein positive tumor cells for Ku70 can identify patients with high probability of response to induction chemotherapy and longer local recurrence-free survival, leading to longer overall survival. These patients would benefit from a conservative treatment based on chemoradiotherapy or radiotherapy and would differ from those who would not respond and would require surgical resection or the exploration of alternative therapies.

Acknowledgements

References

1. Pfister DG, Laurie SA, Weinstein GS, Mendenhall WM, Adelstein DJ, Ang KK, Clayman GL, Fisher SG, Forastiere AA, Harrison LB, Lefebvre JL, Leupold N, et al. American Society of Clinical Oncology clinical practice guideline for the use of larynx-preservation strategies in the treatment of laryngeal cancer. J Clin Oncol 2006;24:3693–704.
2. Lamont EB, Vokes EE. Chemotherapy in the management of squamous-cell carcinoma of the head and neck. Lancet Oncol 2001;2:261–9.
3. Posner MR, Haddad RI, Wirth L, Norris CM, Goguen LA, Mahadevan A, Sullivan C, Tishler RB. Induction chemotherapy in locally advanced squamous cell cancer of the head and neck: evolution of the sequential treatment approach. Semin Oncol 2004;31:778–85.
4. Ensley JF, Jacobs JR, Weaver A, Kinzie J, Crissman J, Kish JA, Cummings G, Al-Sarraf M. Correlation between response to cisplatinum-combination chemotherapy and subsequent radiotherapy in previously untreated patients with advanced squamous cell cancers of the head and neck. Cancer 1984;54:811–4.
5. Spaulding MB, Fischer SG, Wolf GT. Tumor response, toxicity, and survival after neoadjuvant organ-preserving chemotherapy for advanced laryngeal carcinoma. The Department of Veterans Affairs Cooperative Laryngeal Cancer Study Group. J Clin Oncol 1994;12:1592–9.
6. Altundag O, Gullu I, Altundag K, Yalcin S, Ozyar E, Cengiz M, Akyol F, Yucel T, Hosal S, Sozeri B. Induction chemotherapy with cisplatin and 5-fluorouracil followed by chemoradiotherapy or radiotherapy alone in the treatment of locoregionally advanced resectable cancers of the larynx and hypopharynx: results of single-center study of 45 patients. Head Neck 2005;27:15–21.
7. Patel SG, Shah JP. TNM staging of cancers of the head and neck: striving for uniformity among diversity. CA Cancer J Clin 2005;55:242–58; quiz 61–2, 64.
8. Sorenson CM, Eastman A. Mechanism of *cis*-diamminedichloroplatinum(II)-induced cytotoxicity: role of G2 arrest and DNA double-strand breaks. Cancer Res 1988;48:4484–8.
9. Whitaker SJ, Powell SN, McMillan TJ. Molecular assays of radiation-induced DNA damage. Eur J Cancer 1991;27:922–8.
10. Yoshioka A, Tanaka S, Hiraoka O, Koyama Y, Hirota Y, Ayusawa D, Seno T, Garrett C, Wataya Y. Deoxyribonucleoside triphosphate imbalance. 5-Fluorodeoxyuridine-induced DNA double strand breaks in mouse FM3A cells and the mechanism of cell death. J Biol Chem 1987;262:8235–41.
11. McHugh PJ, Sones WR, Hartley JA. Repair of intermediate structures produced at DNA interstrand cross-links in *Saccharomyces cerevisiae*. Mol Cell Biol 2000;20:3425–33.
12. Haber JE. Partners and pathwaysrepairing a double-strand break. Trends Genet 2000;16:259–64.
13. Korabiowska M, Voltmann J, Honig JF, Bortkiewicz P, Konig F, Cordon-Cardo C, Jenckel F, Ambrosch P, Fischer G. Altered expression of DNA double-strand repair genes Ku70 and Ku80 in carcinomas of the oral cavity. Anticancer Res 2006;26:2101–5.
14. Gollin SM. Chromosomal alterations in squamous cell carcinomas of the head and neck: window to the biology of disease. Head Neck 2001;23:238–53.
15. Shin KH, Kang MK, Kim RH, Kameta A, Baluda MA, Park NH. Abnormal DNA end-joining activity in human head and neck cancer. Int J Mol Med 2006;17:917–24.
16. Peters GJ, van Triest B, Backus HH, Kuiper CM, van der Wilt CL, Pinedo HM. Molecular downstream events and induction of thymidylate synthase in mutant and wild-type p53 colon cancer cell lines after treatment with 5-fluorouracil and the thymidylate synthase inhibitor raltitrexed. Eur J Cancer 2000;36:916–24.
17. van Gent DC, Hoeijmakers JH, Kanaar R. Chromosomal stability and the DNA double-stranded break connection. Nat Rev Genet 2001;2:196–206.
18. Ferguson DO, Sekiguchi JM, Chang S, Frank KM, Gao Y, DePinho RA, Alt FW. The nonhomologous end-joining pathway of DNA repair is required for genomic stability and the suppression of translocations. Proc Natl Acad Sci USA 2000;97:6630–3.
19. Peng Y, Zhang Q, Nagasawa H, Okayasu R, Liber HL, Bedford JS. Silencing expression of the catalytic subunit of DNA-dependent protein kinase by small interfering RNA sensitizes human cells for radiation-induced chromosome damage, cell killing, and mutation. Cancer Res 2002;62:6400–4.
20. Tian X, Chen G, Xing H, Weng D, Guo Y, Ma D. The relationship between the down-regulation of DNA-PKcs or Ku70 and the chemosensitization in human cervical carcinoma cell line HeLa. Oncol Rep 2007;18:927–32.
21. Salles B, Calsou P, Frit P, Muller C. The DNA repair complex DNA-PK, a pharmacological target in cancer chemotherapy and radiotherapy. Pathol Biol (Paris) 2006;54:185–93.
22. Chu G. Double strand break repair. J Biol Chem 1997;272:24097–100.
23. Brown KD, Lataxes TA, Shangary S, Mannino JL, Giardina JF, Chen J, Baskaran R. Ionizing radiation exposure results in up-regulation of Ku70 via a p53/ataxia-telangiectasia-mutated protein-dependent mechanism. J Biol Chem 2000;275:6651–6.
24. Jensen R, Glazer PM. Cell-interdependent cisplatin killing by Ku/DNA-dependent protein kinase signaling transduced through gap junctions. Proc Natl Acad Sci USA 2004;101:6134–9.
25. Espinosa E, Vara JA, Redondo A, Sanchez JJ, Hardisson D, Zamora P, Pastrana FG, Cejas P, Martinez B, Suarez A, Calero F, Baron MG. Breast cancer prognosis determined by gene expression profiling: a quantitative reverse transcriptase polymerase chain reaction study. J Clin Oncol 2005;23:7278–85.
26. Livak KJ, Schmittgen TD. Analysis of relative gene expression data using real-time quantitative PCR and the 2(-Delta Delta C(T)) method. Methods 2001;25:402–8.
27. Nieuwenhuis EJ, Jaspars LH, Castelijns JA, Bakker B, Wishaupt RG, Denkers F, Leemans CR, Snow GB, Brakenhoff RH. Quantitative molecular detection of minimal residual head and neck cancer in lymph node aspirates. Clin Cancer Res 2003;9:755–61.
28. Castleman KR. Concepts in imaging and microscopy: color image processing for microscopy. Biol Bull 1998;194:100–7.
29. Maximova OA, Taffs RE, Pomeroy KL, Piccardo P, Asher DM. Computerized morphometric analysis of pathological prion protein deposition in scrapie-infected hamster brain. J Histochem Cytochem 2006;54:97–107.
30. Therasse P, Arbuck SG, Eisenhauer EA, Wanders J, Kaplan RS, Rubinstein L, Verweij J, Van Glabbeke M, van Oosterom AT, Christian MC, Gwyther SG. New guidelines to evaluate the response to treatment in solid tumors. European Organization for Research and Treatment of Cancer, National Cancer Institute of the United States, National Cancer Institute of Canada. J Natl Cancer Inst 2000;92:205–16.
31. Layland MK, Sessions DG, Lenox J. The influence of lymph node metastasis in the treatment of squamous cell carcinoma of the oral cavity, oropharynx, larynx, and hypopharynx: N0 versus N+. Laryngoscope 2005;115:629–39.
32. Hasina R, Lingen MW. Head and neck cancer: the pursuit of molecular diagnostic markers. Semin Oncol 2004;31:718–25.
33. Panis X, Coninx P, Nguyen TD, Legros M. Relation between responses to induction chemotherapy and subsequent radiotherapy in advanced or multicentric squamous cell carcinomas of the head and neck. Int J Radiat Oncol Biol Phys 1990;18:1315–8.
34. Bjork-Eriksson T, West C, Nilsson A, Magnusson B, Svensson M, Karlsson E, Slevin N, Lewensohn R, Mercke C. The immunohistochemical expression of DNA-PKCS and Ku (p70/p80) in head and neck cancers: relationships with radiosensitivity. Int J Radiat Oncol Biol Phys 1999;45:1005–10.
35. Shintani S, Mihara M, Li C, Nakahara Y, Hino S, Nakashiro K, Hamakawa H. Up-regulation of DNA-dependent protein kinase correlates with radiation resistance in oral squamous cell carcinoma. Cancer Sci 2003;94:894–900.

36. Noguchi T, Shibata T, Fumoto S, Uchida Y, Mueller W, Takeno S. DNA-PKcs expression in esophageal cancer as a predictor for chemoradiation therapeutic sensitivity. Ann Surg Oncol 2002;9:1017–22.

37. Friesland S, Kanter-Lewensohn L, Tell R, Munck-Wikland E, Lewensohn R, Nilsson A. Expression of Ku86 confers favorable outcome of tonsillar carcinoma treated with radiotherapy. Head Neck 2003;25:313–21.

38. Lee SW, Cho KJ, Park JH, Kim SY, Nam SY, Lee BJ, Kim SB, Choi SH, Kim JH, Ahn SD, Shin SS, Choi EK, et al. Expressions of Ku70 and DNA-PKcs as prognostic indicators of local control in nasopharyngeal carcinoma. Int J Radiat Oncol Biol Phys 2005;62:1451–7.

39. Spano JP, Busson P, Atlan D, Bourhis J, Pignon JP, Esteban C, Armand JP. Nasopharyngeal carcinomas: an update. Eur J Cancer 2003;39:2121–35.

40. Wilson CR, Davidson SE, Margison GP, Jackson SP, Hendry JH, West CM. Expression of Ku70 correlates with survival in carcinoma of the cervix. Br J Cancer 2000;83:1702–6.

41. Harima Y, Sawada S, Miyazaki Y, Kin K, Ishihara H, Imamura M, Sougawa M, Shikata N, Ohnishi T Expression of Ku80 in cervical cancer correlates with response to radiotherapy and survival. Am J Clin Oncol 2003;26:e80–e85.

42. Olaussen KA, Dunant A, Fouret P, Brambilla E, Andre F, Haddad V, Taranchon E, Filipits M, Pirker R, Popper HH, Stahel R, Sabatier L, et al. DNA repair by ERCC1 in non-small-cell lung cancer and cisplatin-based adjuvant chemotherapy. N Engl J Med 2006;355:983–91.

43. Dabholkar M, Bostick-Bruton F, Weber C, Bohr VA, Egwuagu C, Reed E. ERCC1 and ERCC2 expression in malignant tissues from ovarian cancer patients. J Natl Cancer Inst 1992;84:1512–7.

44. Smith GC, Jackson SP. The DNA-dependent protein kinase. Genes Dev 1999;13:916–34.

45. Gao Y, Chaudhuri J, Zhu C, Davidson L, Weaver DT, Alt FW. A targeted DNA-PKcs-null mutation reveals DNA-PK-independent functions for KU in V(D)J recombination. Immunity 1998;9:367–76.

46. Dip R, Naegeli H. More than just strand breaks: the recognition of structural DNA discontinuities by DNA-dependent protein kinase catalytic subunit. FASEB J 2005;19:704–15.

47. Takata M, Sasaki MS, Sonoda E, Morrison C, Hashimoto M, Utsumi H, Yamaguchi-Iwai Y, Shinohara A, Takeda S. Homologous recombination and non-homologous end-joining pathways of DNA double-strand break repair have overlapping roles in the maintenance of chromosomal integrity in vertebrate cells. EMBO J 1998;17:5497–508.

48. Wang S, Guo M, Ouyang H, Li X, Cordon-Cardo C, Kurimasa A, Chen DJ, Fuks Z, Ling CC, Li GC. The catalytic subunit of DNA-dependent protein kinase selectively regulates p53-dependent apoptosis but not cell-cycle arrest. Proc Natl Acad Sci USA 2000;97:1584–8.

49. Woo RA, Jack MT, Xu Y, Burma S, Chen DJ, Lee PW. DNA damage-induced apoptosis requires the DNA-dependent protein kinase, and is mediated by the latent population of p53. EMBO J 2002;21:3000–8.

50. Jack MT, Woo RA, Hirao A, Cheung A, Mak TW, Lee PW. Chk2 is dispensable for p53-mediated G1 arrest but is required for a latent p53-mediated apoptotic response. Proc Natl Acad Sci USA 2002;99:9825–9.

51. Jack MT, Woo RA, Motoyama N, Takai H, Lee PW. DNA-dependent protein kinase and checkpoint kinase 2 synergistically activate a latent population of p53 upon DNA damage. J Biol Chem 2004;279:15269–73.

52. Cobb LJ, Liu B, Lee KW, Cohen P. Phosphorylation by DNA-dependent protein kinase is critical for apoptosis induction by insulin-like growth factor binding protein-3. Cancer Res 2006;66:10878–84.

53. Yang CR, Leskov K, Hosley-Eberlein K, Criswell T, Pink JJ, Kinsella TJ, Boothman DA. Nuclear clusterin/XIP8, an x-ray-induced Ku70-binding protein that signals cell death. Proc Natl Acad Sci USA 2000;97:5907–12.

54. Zhao HJ, Hosoi Y, Miyachi H, Ishii K, Yoshida M, Nemoto K, Takai Y, Yamada S, Suzuki N, Ono T. DNA-dependent protein kinase activity correlates with Ku70 expression and radiation sensitivity in esophageal cancer cell lines. Clin Cancer Res 2000;6:1073–8.

55. Deriano L, Guipaud O, Merle-Beral H, Binet JL, Ricoul M, Potocki-Veronese G, Favaudon V, Maciorowski Z, Muller C, Salles B, Sabatier L, Delic J. Human chronic lymphocytic leukemia B cells can escape DNA damage-induced apoptosis through the nonhomologous end-joining DNA repair pathway. Blood 2005;105:4776–83.

56. Gu Y, Jin S, Gao Y, Weaver DT, Alt FW. Ku70-deficient embryonic stem cells have increased ionizing radiosensitivity, defective DNA end-binding activity, and inability to support V(D)J recombination. Proc Natl Acad Sci USA 1997;94:8076–81.

57. Gudkov AV, Komarova EA. The role of p53 in determining sensitivity to radiotherapy. Nat Rev Cancer 2003;3:117–29.

58. Panta GR, Kaur S, Cavin LG, Cortes ML, Mercurio F, Lothstein L, Sweatman TW, Israel M, Arsura M. ATM and the catalytic subunit of DNA-dependent protein kinase activate NF-kappaB through a common MEK/extracellular signal-regulated kinase/p90(rsk) signaling pathway in response to distinct forms of DNA damage. Mol Cell Biol 2004;24:1823–35.

59. Nueda A, Hudson F, Mivechi NF, Dynan WS. DNA-dependent protein kinase protects against heat-induced apoptosis. J Biol Chem 1999;274:14988–96.

60. Tai YT, Podar K, Kraeft SK, Wang F, Young G, Lin B, Gupta D, Chen LB, Anderson KC. Translocation of Ku86/Ku70 to the multiple myeloma cell membrane: functional implications. Exp Hematol 2002;30:212–20.

61. Rooney S, Alt FW, Lombard D, Whitlow S, Eckersdorff M, Fleming J, Fugmann S, Ferguson DO, Schatz DG, Sekiguchi J. Defective DNA repair and increased genomic instability in Artemis-deficient murine cells. J Exp Med 2003;197:553–65.

62. Jin S, Inoue S, Weaver DT. Differential etoposide sensitivity of cells deficient in the Ku and DNA-PKcs components of the DNA-dependent protein kinase. Carcinogenesis 1998;19:965–71.

63. Cabelguenne A, Blons H, de Waziers I, Carnot F, Houllier AM, Soussi T, Brasnu D, Beaune P, Laccourreye O, Laurent-Puig P. p53 alterations predict tumor response to neoadjuvant chemotherapy in head and neck squamous cell carcinoma: a prospective series. J Clin Oncol 2000;18:1465–73.

64. Rusch V, Klimstra D, Venkatraman E, Oliver J, Martini N, Gralla R, Kris M, Dmitrovsky E. Aberrant p53 expression predicts clinical resistance to cisplatin-based chemotherapy in locally advanced non-small cell lung cancer. Cancer Res 1995;55:5038–42.

65. Bergh J, Norberg T, Sjogren S, Lindgren A, Holmberg L. Complete sequencing of the p53 gene provides prognostic information in breast cancer patients, particularly in relation to adjuvant systemic therapy and radiotherapy. Nat Med 1995;1:1029–34.

66. Buttitta F, Marchetti A, Gadducci A, Pellegrini S, Morganti M, Carnicelli V, Cosio S, Gagetti O, Genazzani AR, Bevilacqua G. p53 alterations are predictive of chemoresistance and aggressiveness in ovarian carcinomas: a molecular and immunohistochemical study. Br J Cancer 1997;75:230–5.

67. Eid H, Van der Looij M, Institoris E, Geczi L, Bodrogi I, Olah E, Bak M. Is p53 expression, detected by immunohistochemistry, an important parameter of response to treatment in testis cancer? Anticancer Res 1997;17:2663–9.

68. Tada M, Matsumoto R, Iggo RD, Onimaru R, Shirato H, Sawamura Y, Shinohe Y. Selective sensitivity to radiation of cerebral glioblastomas harboring p53 mutations. Cancer Res 1998;58:1793–7.

69. Cote RJ, Esrig D, Groshen S, Jones PA, Skinner DG. p53 and treatment of bladder cancer. Nature 1997;385:123–5.

70. Koch WM, Brennan JA, Zahurak M, Goodman SN, Westra WH, Schwab D, Yoo GH, Lee DJ, Forastiere AA, Sidransky D. p53 mutation and locoregional treatment failure in head and neck squamous cell carcinoma. J Natl Cancer Inst 1996;88:1580–6.

71. Fakhry C, Gillison ML. Clinical implications of human papillomavirus in head and neck cancers. J Clin Oncol 2006;24:2606–11.